SEBHA UNIVERSITY JOURNAL OF PURE & APPLIED SCIENCES VOL.22 NO. 1 2023
DOI: 10.51984/JOPAS.V22I1.1456

مجلة جامعة سبها للعلوم البحتة والتطبيقية
Sebha University Journal of Pure & Applied Sciences

Journal homepage: www.sebhau.edu.ly/journal/index.php/jopas

# Review: Electrochemical biosensors based on ZnO nanostructures

M. Akhwater

Department of physics, College of Arts and Sciences/University of Benghazi, EL Marj, Libya

**Keywords:**
Biosensors
Cholesterol
Electrochemical
Glucose
ZnO nanostructures

**ABSTRACT**

In the last few decades' electrochemical biosensors have witnessed vast developments due to the broad range of different applications, including health care and medical diagnosis, environmental monitoring and assessment, food industry, and drug delivery. Integration of nanostructured material with different disciplines and expertise of electrochemistry, solid-state physics, material science, and biology has offered the opportunity of a future generation of highly rapid, sensitive, stable, selective, and novel electrochemical biosensor devices.

Among metal oxide nanomaterials, ZnO nanostructures are one of the most important nanomaterials in today's nanotechnology research. Such nanostructures have been studied intensely not only for their extraordinary structural, optical, and electronic properties but also for their prominent performance in diverse novel applications such as photonics, optics, electronics, drug delivery, cancer treatment, bio-imaging, etc. However, functionality of these nanomaterials is eventually dictated by the capability to govern their properties including shape, size, position, and crystalline structure on the nanosized scale.

This review aims to update the outstanding advancement in the developments of the enzymatic and non-enzymatic biosensors using a different structure of ZnO nanomaterials. After a coverage of the basic principles of electrochemical biosensors, we highlight the basic features of ZnO as a potential anticancer agent. focused attention gives to functionalized biosensors based on ZnO nanostructures for detecting biological analytes, such as glucose, cholesterol, L-lactic acid, uric acid, metal ions, and pH.

## مراجعة : أجهزة الاستشعار الحيوية الكهروكيميائية القائمة على البنية النانوية لأكسيد الزنك

مريم اخويطر

قسم الفيزياء، كلية الآداب والعلوم المرج، جامعة بنغازي، ليبيا

**الكلمات المفتاحية:**
أجهزة الاستشعار الحيوية
الكوليسترول
الكهروكيميائية
الجلوكوز
التراكيب النانوية لأكسيد الزنك

**الملخص**

شهدت أجهزة الاستشعار الحيوية الكهروكيميائية على مدى العقد الماضي تطورات واسعة النطاق بسبب تطبيقاتها الواسعة والمختلفة، بما في ذلك الرعاية الصحية والتشخيص الطبي، والرصد والتقييم البيئيين، وصناعة الأغذية، وتوصيل الأدوية داخل الأعضاء الحيوية للجسم البشري. وقد أتاح دمج المواد النانوية مع مختلف التخصصات والخبرات في الكيمياء الكهربائية، وفيزياء الحالة الصلبة، وعلوم المواد، والبيولوجيا فرصة لبناء جيل المستقبل من أجهزة الاستشعار الحيوية الكهروكيميائية التي تتمتع بالسرعة، والحساسية، والاستقرار، والانتقائية. من بين العديد من المواد التي تم دراستها، تم تحديد البنية النانوية لأكسيد الزنك (ZnO)كمرشح واعد لأجهزة الاستشعار الحيوي بسبب ميزاتها التركيبية والبصرية والكهربائية الفريدة .

يهدف هذا العمل إلى عرض التقدم البارز في تطورات أجهزة الاستشعار الحيوية الأنزيمية وغير الأنزيمية المبنية على أساس التراكيب النانوية لأكسيد الزنك. بعد مناقشة المبادئ الأساسية لأجهزة الاستشعار الحيوية الكهروكيميائية تم تسليط الضوء على الدور الأساسي لأكسيد الزنك كعامل مساعد لعلاج السرطان. أيضا تم تركيز الاهتمام على أنظمة الاستشعار الحيوية الوظيفية القائمة على التراكيب النانوية لأكسيد الزنك والمستخدمة في الكشف عن التحليلات البيولوجية، بما في ذلك الجلوكوز والكوليسترول وحمض اللاكتيك وحمض اليوريك وأيونات المعادن، ومستويات الحامضية.

*Corresponding author:
E-mail addresses: mary44772@yahoo.com
*Article History : Received 16 September 2021 - Received in revised form 04 March 2023 - Accepted 18 March 2023*

**Introduction**

Over the past decades, key technological developments in biosensors fabrication have been intensively witnessed. Biosensors are categorized according to the detection concepts into various biosensor platforms such as photometric, calorimetric, electrochemical, piezoelectric, etc. They are highly used in medical, chemical, and biological applications, environmental monitoring tools, and food processing [1]. Due to the analysis of biological or biochemical responses is extremely critical for medical, biological and biotechnological applications, it is quite challenging to transform the biological interactions to easily manipulated electronic signals because of the intricacy of a direct connection between an electronic platform and a biological environment [2].

However, electrochemical biosensors are applicable for high-volume production and offered a significant level of detection because of the reliable adaptation of a biological response to an electronic signal with excellent stability. Other constitutional benefits of electrochemical biosensors are their stability, simple diminishment, superlative determination limits with less analyte volumes. In comparison to spectroscopic-based approaches, electrochemical processes did not influence by biofluids turbidity, quenching, or interference from absorbing and fluorescing compounds usually found in biological specimens [3, 4]. However, improvement of a sensitivity level and precise identification of the bioanalytical responses of the desired biomolecules have still undergone to a deficiency of surface morphology. For an instant, a change of PH and the ion concentration in biofluids can affect the responses of some biosensors like immunosensors [4]. Hence, a significant effort has currently been executed to minimize the dimension of biosensor compounds, attempting to improve the ratio of signal power to the noise power for biosensors, e.g., using various enzymatic labels to facilitate detection and boost the output of the interesting event [2].

In this work, we shed light on the magnificent developments of different enzymatic and non-enzymatic biosensors which have been fabricated using a various morphology of ZnO nanomaterials. In general, the target of these novel bioanalytical platforms is to measure output signal response for diagnostic, therapeutic, and medical objectives when a biological recognition component interacts with the transducing surface. A biorecognition component usually defines as a biomarker, which is a biomolecule that represents the pathophysiological state such as abnormality in the regulation of the cellular functions, pathological reactions, or intervention to any therapeutic drugs. Different biological components are described as bioreceptors (e.g., enzymes, nucleic acids, Immune protein and so on) are applied to observe biomarkers. Biomarkers consider as an essential indication in diagnosing many diseases [5]. Some effective techniques to determine these biomarkers including, screening the biological fluids for expressing any proteins, DNA or ribonucleic acid (RNA) expression profiles, circulating tumour cells, lipids, metabolites, etc. [5].

The biosensor production involves two essential sections of bioanalytical platforms: traditional devices that include testing in clinical laboratories services where expensive instruments for examination, a requirement to training qualified staff for laboratory placing the high burden of health care cost on patients [6,7] and low-priced, practical, and easy-to-carry point-of-care (POC) devices for testing in both clinical and non-clinical health care [8,9]. Fabrication and advancement of POC biosensors have drawn tremendous attention in many medical, biological applications as it helps patients and psychiatrists to perform testing in the distance at the patient home care and supplies critical data almost instantly [9].

The biosensors have rapidly grown to be a thriving research area because of the continuing growth of diseases and significant demand for modern, portable healthcare equipment's. Developments in nanomaterials and nanoscience have allowed improving conventional biosensor design. The basic obstacles to accomplish a high-quality biosensor is selectivity which is the capability to differentiate relevant biomarkers over various biomolecules and proteins existing in the biological fluid. Also, the sensitivity expresses the capability to identify relevant bio-markers at comparably small concentrations (typically in lower pg/ml) without interferences with other biomolecules. Moreover, other requirements require to be addressed, such as low signal-to-noise ratio of readout mechanism, the lower detection limit, minimization of the specimen size, long-term monitoring, and rapid and precise detection [10]. The following section focuses on fundamental principles that have been utilised to design different biosensor devices.

**2. Basic principles of electrochemical biosensors**

Advanced methodologies and techniques in nanofabrication have made it achievable to design practical, reliable, and stable biosensor devices. Miniaturizing the dimension of biosensor to the nanoscale allows studying different targeted biomolecules interacting under the same biological condition, thus lowering the sensing process cost and significantly increasing the throughput. However, the efficient performance of miniaturized biosensors is highly affected by the transduction mechanism. For instant, in electrical/electrochemical biosensors, transduction of physiochemical alterations is uncomplicated and durable, which allow miniaturizing limited resources while, in optical biosensors, transduction provides reduction signal intervention from other biological species [11]. However, the fabrication of highly performed biosensor devices has been driven by its sensitivity and selectivity, stability and most essentially biocompatibility of the selected component.

Current advancements in material technology and nanoscience have provided a new age of nano biological and healthcare sensors to be an intensely bright research area. Nanomaterials possess various advantages over bulk materials including a broad surface-to-volume ratio which enhances the sensitivity for detecting targeted analytes in their biological surroundings. However, biological medium or fluid contains many different analytes which could interfere with specific detection [12]. Thus, another significant aspect that should be regarded through the biosensor design is the selectivity to a desired analyte, where surface functionalization becomes so significant. Hence, the basic strategies to follow during the biosensor design procedure include, choosing the appropriate transduction materials to fabricate bio-interfaces, surface modification chemistry of substrates to grasp the nature of the immobilized biomolecules, modification of physicochemical structural characteristics to develop determinable real-time signal with lower signal-to-noise ratio and, lastly, integrating electronics, material science, nanofabrication, and biology to create extremely powerful and smart biosensor [12].

The selection criterion of several materials e.g., semiconducting metals/metal oxides, polymers/ceramics, hydrogels, and so on, to achieve highly performed and applicable biosensor for a specific platform is extremely important [2]. Polymer material needs intensive surface treatment due to its lack of chemical moieties for surface functionalization however, these complicated processes could influence the polymer surface changing its features causing nonspecific interaction of biomolecules [13]. Nanomaterials with a scale less than a few hundred nm, several orders of magnitude smaller than human cells, can show distinctive properties that differ from those in macro or bulkier structures and exhibit unique interactions with biomolecules both on the inside and outside of the biological surroundings [14, 15].

Therefore, the most preferred materials to design highly performed biosensor devices are nanomaterials such as nanoparticles, nanorods, nanowires, etc. [16,17]. These materials offer extraordinary characteristics and extend surface exposed area for biomolecular binding. The biosensor design process significantly influences by the shape and structure of nanomaterial surfaces which help transducing the physiochemical changes to biomolecular binding. The topographical features of nanomaterial can modify to match a biomolecule size. Nanomaterial and its structures synthesized from metal oxides of $TiO_2$, CNT- $TiO_2$, $SnO_2$, $ZrO_2$, etc., have been applied

to design glucose oxidase (GOx), cholesterol oxidase and other enzymatic biosensors [18, 19].

The essential aim of the biosensing process is to produce an accurate and rapid identification of the bio species with high sensitivity and selectivity. Fig. 1 illustrates the fundamental elements of the electrochemical biosensor. The first element is the analyte which is the targeted biomolecule including glucose, uric acid, cholesterol, and DNA. The second element is the bioreceptor which is biomolecules such as enzyme, DNA, protein, cell, antibodies, and antigens that capture the bio analytes and bind to them. Third, the transducer component is an interface design where specific biological interactions occur and create a physical response which might be optical, chemical, electrical, thermal, mechanical, etc. Then, those signals convert to highly sensitive electronic signals with lowest disruption by the transducer. Lastly, signals process by software packages to be changed to a significant physical parameter clarifying the analysed procedure [20].

In electrochemical biosensors, the quantification process to derive data about the biological or biochemical system is usually electrochemical, by which a bio-electrochemical component reacts as the basic transduction unit that directly transforms the biological interactions to electronic/electric responses [21]. Usually, the reaction of the biological or biochemical system under study could produce a quantitative current (amperometric), a quantitative potential (potentiometric), or partly change the conduction of conditions (conductometric) between electrodes [21]. Amperometric techniques are electrochemical biosensors commonly known as 'enzyme electrodes' that continually determine current generating by the oxidation or reduction of an electrically effective component in the biochemical event [22, 23].

Usually, amperometry indicates the estimation of the electrical current at a stable potential, while the average current during controlled changes of the potential is identified as voltammetry that is the fundamental mechanism of cyclic voltammetry analysis. These biosensors integrate the analytical influence of electrochemistry with the specificity of biological catalysts such as enzymes for a particular type of chemical bond or functional group [21]. Moreover, a maximum of the measured electric currents escalated straightly with the density of the analyte species in a scale of linear potential [ 21, 22]. However, not all biological species are inherently able to serve as redox participants in electrochemical interactivities, therefore these biosensors use redox mediators to facilitate the electron transfer process at electrode facets [21, 23]. Although the downside of such indirect detection performance of amperometric devices, they are still preferred, and their sensitivity is commonly higher compared to potentiometric devices [24].

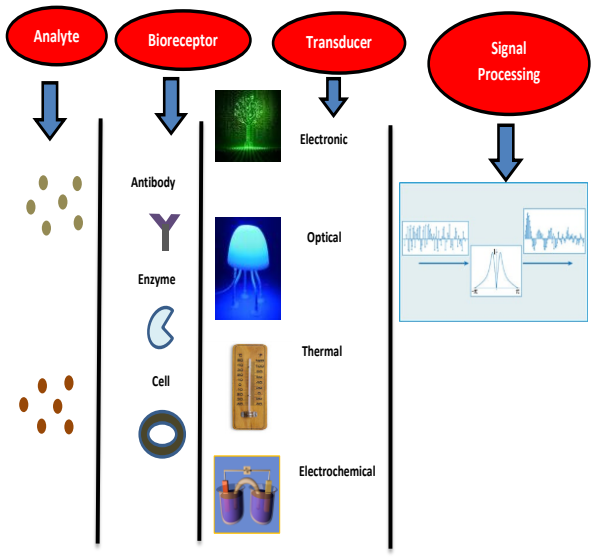


**Figure. 1:** Illustration of the main units of the electrochemical biosensor [20].

In general, potentiometric techniques are electrochemical analysis methods that measure the electrical potential (voltage) between working and reference electrodes under the condition of zero external current flow to give the concentration of anionic analyte in an analytical cell [4,22]. The determination of potentiometry is subjected to the Nernst equation which, describes the connection among the potential differences and the concentration. The straightforward measurement of the ion density by the Nernst equation is also described as direct potentiometry [25]. Another similar method recognized as potentiometric titration has been applied to electrically identify the point at which equivalent amounts of different solutions approach an equilibrium condition. During this process, the amount of a sample determines by introducing evaluated increments of titrant until the endpoint, at which essentially all the reacted sample is identified. The titration process is post-dated via quantifying the potential variation between working and reference electrodes which generate by the differences of the density of an ionic solution at constant or no significant current net to keep the state of thermodynamic equilibrium [2]. Other potentiometric techniques are also established on several structures of field-effect transistor (FET) instruments for identifying pH variations, selective ion densities and enzyme reaction kinetics [26].
Finally, the conductometric measurement methods which can classify as a branch of electrochemical impedance spectroscopy for determining capacitance variations. Typically, they measure the capability of an electrolyte solution to generate electrically conductive surroundings. The conductivity of analytes produces by the decomposition of the dissolved materials (e.g., electrolyte), into ions which migrate and induce by an electrical field thus, the electrolyte current generates by the ion's flow to the electrodes where it becomes neutral [27]. Mostly conductometric techniques have employed to analyse enzymatic interactions which cause variations in the density of charged particles into the fluid [4]. Conductometric biosensors have integrated with nanostructures, especially nanowires [28, 29]. There are different outstanding applications of these methods including, drug detection in human urine and environmental pollution monitoring [30]. The following section provides details on the significance of the ZnO nanostructures as potential and effective agent for cancer prevention and therapeutics.

### 3. ZnO as promising anticancer agent

ZnO has hugely become a topic of interest in the past decade because of its distinctive functional and physicochemical features. ZnO classifies as an inorganic II-VI semiconductor with a direct large bandgap energy of 3.37 eV in the near UV spectral region and a broad

exciton binding energy of 60 meV [31, 32]. As a large bandgap semiconductor, ZnO can endure high temperatures, larger electric fields, higher sparking potential, and high-power operation [31]. ZnO has high thermal and mechanical stability at room temperature, which enables it to be a capable material to be employed in optoelectronics and electronics applications [33, 34, 35]. Besides, due to its piezo and pyroelectric characteristics, ZnO could be employed as a photocatalyst, converter, sensor, and energy generator in hydrogen production [36, 37]. During the past several decades, bioanalytical chemistry and medical diagnostics have witnessed a radical change because of the enormous evolution in nanotechnology. All required and appealing physicochemical properties that needed for prospering biomedical applications offered by ZnO nanostructures. These extraordinary materials are superior candidates as biocompatible and biodegradable nanoplatforms for cancer-targeted imaging and therapy and optical imaging and magnetic resonance imaging (MRI) in cells [38].

Inherently, zinc is considered as one of the most key materials in the human health and nutrition. It plays a fundamental role in the immunity system, influencing many features of humoral and cellular immune responses [38]. Chemically, the ZnO surface has a lot of -OH groups, that could be directly adjusted by various surface patterns of different molecules [39, 40]. ZnO can also gradually decompose in acidic conditions like tumour cells and intense alkaline ambiences if the surface is in direct connection with the biofluid [41]. Additionally, the ZnO nanowires can be dissolved by the biofluid and absorbed by the body to be involved in the nutritional cycle without causing any obstruction [41]. Thus, ZnO regulates several cellular functions of the human body and preserve essential cellular homoeostasis [42]. Furthermore, zinc plays a significant role in oxidative stress process, deoxyribonucleic acid (DNA) replication, DNA damage and repair, cell cycle progression and programmed cell death (apoptosis).

In the case that a cell undergoes any condition of malignancy, a DNA repair mechanism is activated to repair the alteration in the chemical structure of DNA [42]. When this process cannot correct the DNA damage, the cell experiences programmed cell death (apoptosis) to inhibit the division of changed cells, which could then evolve in the cancerous cell. In whatever way, zinc participates in all these crucial mechanisms to protect cells against cancer, and a lack of cellular zinc can cause DNA damage, leading to failing the integrity and stability of DNA and increasing the likelihood of cancer disease [42]. Altos of literature has suggested that a deficiency in zinc concentration or alteration of zinc concentration is a critical symptom of several cancer diseases. Over the past several decades, cancer, a condition of uncontrolled growth of the cell, has been treated by chemotherapy, radiation therapy, Photodynamic therapy, and surgery [43]. These remedial treatments are assuredly efficient in the demolition of cancerous cells but, they have an unfavourable impact because of their unselective reaction towards normal cells too [25]. Owing to the breakthrough of nanomedicine, targeted drug delivery systems and multi-target inhibitor approaches, these traditional cancer therapeutics have gradually become out-of-date techniques [44].

Biomedical applications are opening doors for early detection and treatment of cancer through engineered nanostructures that provide many benefits such as active, and passive targeted delivery, superlative solubility, bioavailability, biocompatibility, and multifunctionality [45]. In addition, due to the diameter dimension of the nanowires is less than that of cells and biomolecules, including DNA, RNA, circulating tumour cells (CTCs), and proteins, the nanowire tip can pass through and disrupt the cell membrane function, which makes it possible to extract microorganisms in cells faster than in previous conventional approaches [46]. It also allowed scientists to apply nanowires as a probe tip to observe cellular electrical activity and record changes in living biological systems like cells and tissues [47]. ZnO nanomaterial has been broadly using for their anti-cancerous features, its selective cytotoxicity against cancerous cells in in vitro conditions has been investigated by Hanley et al. [48]. It has found that ZnO nanoparticles exhibit a capability to target and kill cancerous cells compared to normal ones, which can reduce the side effects on normal cells. In terms of biomedicine fabrications, the biocompatibility and biodegradability of nanomaterials are always a concerning matter. Fortunately, ZnO has been certified by the food and drug administration and is mainly admitted as harmless for cosmetic uses because of its stability and outstanding capability to absorb UV radiation [38].

Even though extracellular ZnO nanoparticles display biocompatibility, high concentrations of free intracellular zinc induced cytotoxicity in the immune cells of the human body [49]. One of the features of ZnO cytotoxicity against cancerous cells is its capacity to promote reactive oxygen species, resulting in oxidative strain and decisively cellular death when the anti-oxidative efficiency of the cell is exceeded [50]. Other investigations have reported that ZnO nanomaterials were non-poisonous to normal cells and selectively poisonous to bacteria or cancerous cells [51, 48]. Another report has found that ZnO nanowires show cytotoxicity to human monocyte macrophages at specific concentrations, the rapid dissolution of ZnO nanowires in a biofluid, escalating zinc ion density, causing cells to dye [52]. However, many efforts require to estimate the toxicity effect of ZnO nanomaterials to allow these nanomaterials to be safely integrated for future biomedical applications. ZnO nanowire has a large surface to volume ratio owing to its nanoscale, which enables promoting its surface interaction, reactiveness, and solubility. The well-defined architecture of ZnO nanomaterials has high sensitivity with less response time therefore, these attractive physicochemical traits allow ZnO to integrate with micro/ nanochannel for biological and chemical sensing applications [47]. A reduction in wire diameter, leading to an extreme rise in the rate of surface atoms in comparison with internal atoms. Hence, exterior facet contact by charged ions or biological species significantly affects the conduction on the exterior and interior surfaces of the wire. It is critical to describe and study the interactions through the inner atoms based on quantum mechanics theory of wave-like electron transport through the nanowire, rather than classical mechanics theory of ballistic electron transport [53, 54]. It means that the conductivity of the nanowire is contingent on quantum confinement into the separate quantization energy levels. A demonstration of how surface atom interactions affect the nanowire conduction shows in Fig. 2. In the micrometre dimensions, the surface-to-volume area of the wire is comparably small. Once surface atoms interact or bind with other charged ions or bio species, their intercorrelation with biological systems occurs nearby the surface whereas, a large area of the internal atoms remains uncontactable.

While a reduction of the wire dimensionality to the nanometer size, the surface-to-volume ratio significantly extends. Therefore, the wire exterior and interior both can participate in the wire conduction and increase the chance for reactivity, solubility, and many other characteristics of nanowires [2]. Furthermore, ZnO nanomaterials also show other valuable properties for the analytical devices, including high catalytic adeptness, wide electron transfer efficiency, broad adsorption capacity, and high isoelectric point (IEP; ~9.5), which are suited for adsorption of specific proteins like enzymes and antibodies with low (IEPs) by electrostatic interaction [55]. as the IEP of ZnO is significantly greater than the IEP of most biological species which, offers appropriate surroundings for the biomolecule's immobilization process. Hence, biological species are negatively charged owing to a smaller IEP causing to be smoothly immobilized on positively charged ZnO during an extremely active electrostatic interaction. The electrical transport features of ZnO are significantly influenced by the crystalline composition and surface polarity which, could be tailored. Moreover, the strong ionic strength and pH stability enable ZnO to perform with biofluids [56]. The following section sheds light upon the surface functionalization of ZnO nanostructures.

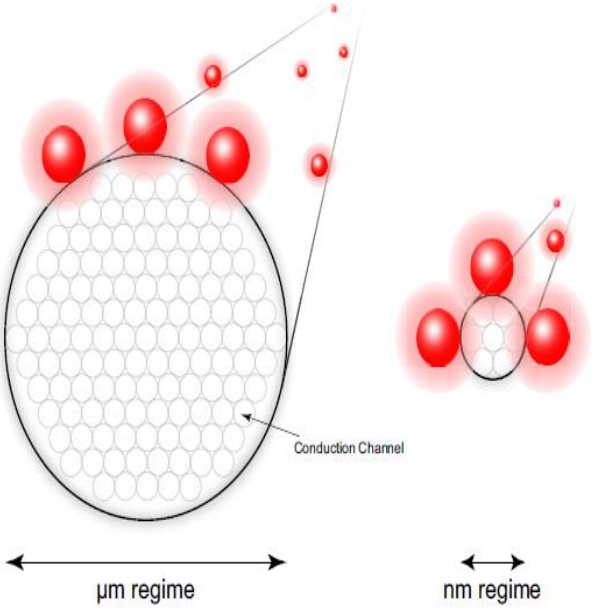


**Figure. 2:** Illustration of the impact of surface to volume ratio in both nm and µm sizes of the wire [2].

**4. Surface functionalization of ZnO**

The overall efficiency and sensibility of electrochemical biosensors are highly affected by the surface functionalization techniques, the different electrochemical transduction processes, and the selection of the immobilizing biorecognition element. The bio-recognition elements are usually surface-immobilized which is considered as a basis to capture the biological analyte molecules which require to be discovered. The successful applications of ZnO nanostructure-based biosensors depend on their specific biological performance and correlation with biological and nano-/microelectronic platforms [2]. Specifically, the size distribution, agglomeration, and morphology of nanostructures and the immobilization procedure of the biorecognition element significantly affect the efficiency of the biosensors. It is critical to build an extremely effective and well-controlled organic/inorganic interface platform for effective charge and energy transfer to produce high sensitivity. In general, the attachment of the biomolecules to the surface can categorize by physical adsorption (e.g., van der Waals, electrostatic, physical adsorption) or chemical binding. In general, enzymes are protein, which might act as an efficient catalyst, and it is also considered as redox enzymes to provide or consume electrons [57]. It utilizes for catalyzing most kinds of chemical and biological reactions in living shrouding therefore, immobilization procedures for enzymes are important to conserve their stability and biological activity [58]. Such Enzymes are perceptive to their conditions, especially their shelf life and operational stability. Inactivation, restriction or unfolding upon adsorption and chemical or thermal inactivation are usual if no specific considerations are used [59]. To keep the enzyme bioactivity, nanomaterials produce a harmonious microenvironment and a wide surface region for higher enzyme loading capacity. Besides, it directly migrates electrons between the electrode and effective point of the enzyme [60,61].

Some electrochemical biosensors use mediators, which are flexible, oxidizer reactants that can employ in case of reactions that occur away from the electrode interface to drive back and forth the electrons between the interaction area and the electrode surface. They response rapidly to the enzyme to oxidize at the electrode facet and reduce at the interaction area of the enzyme or contrariwise. Overall, it is efficient to develop the biochemical reactivity nearby the electrode facet and suppress the distribution of material out of the surface on all sides [62]. In general, electrochemical biosensors are determined by the conception of immediate transduction of the interaction signal into an electric current [21]. In some sensing systems, there is no need to use a mediator because they are subjected to well-defined electron transduction in which the redox enzyme specifically catalyzes the change of a particular substrate so that the electrons straightforwardly travel from the electrode to the substrate molecule or contrariwise [2]. It reported that the direct electron transfer reduces by increasing the space between the electrode facet and the enzyme, causing a reduction in the sensitivity of biosensors [62]. If the indirect transduction takes place, *a mediator* can freely diffuse in solution, communicating with redox enzyme and *shuttling electrons* to the electrode facet, therefore, substantially vast spaces could be reduced (Fig. 3) [21, 63].

The nano-bio interface is a kinetic biophysicochemical reaction among the nanostructured materials and the surface of biological elements, that acts to the dynamic and thermodynamic exchanges among the interfaces [64]. The nano-bio interface consists of three effectively interreacting parts: (a) the nanoparticles' surfaces, where their properties are identified by its physicochemical structure; (b) the solid-liquid interface and the variations which take place when the particle connects to species in the suspending surroundings; (c) the solid-liquid interface's contiguity area with biomolecules and cellular membranes (Fig. 4).

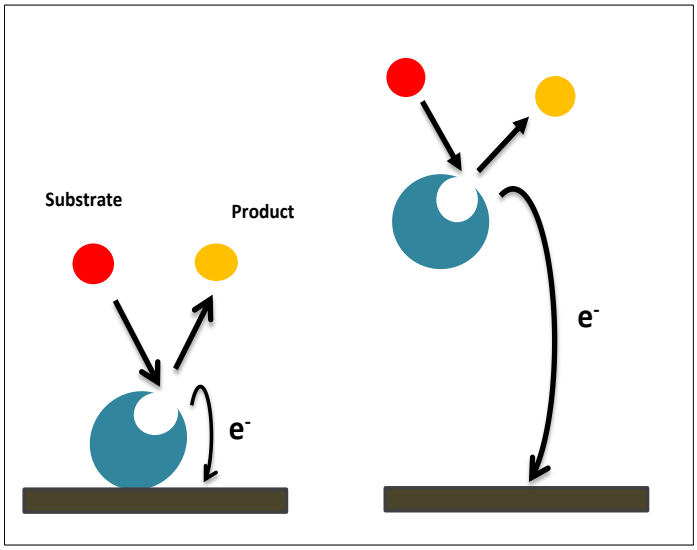


**Figure. 3:** Representation of Direct and Indirect electron transduction [2].

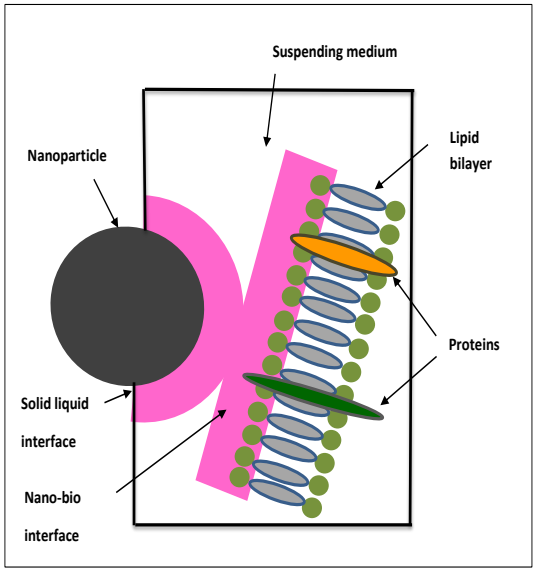


**Figure. 4:** Representation of the interface of a nanoparticle and a lipid bilayer [64].

Another essential interaction that interprets the great significance of nanomaterials in the biological platform is the interaction between nanoparticles themselves [42]. Many different forces including van

der Waals forces, electrostatic force, solvation, solvophobic, and depletion forces are involved in these interactions and influenced the diffusion of nanoparticles in the surrounding [65]. Besides, those forces have a significant function in the adhesion reaction of nanoparticles in the cellular surface and their passive transport across the cell membranes [66, 67]. Hence, it is necessary to comprehend the significance of these interactions to exploit them for healthcare and nanobiological applications.

The following sub-sections introduce a variety of ZnO nanostructures-based biosensors including, glucose biosensors, cholesterol biosensors, L-lactic acid biosensors, uric acid biosensors, metal ion biosensors, and pH biosensors.

### 4. 1. ZnO Nanostructures based Glucose Biosensors

The early stage of ZnO based biosensors was launched by fabricating the first-generation of GOx biosensor in 1962 [68]. Glucose biosensors are still extensively used, e.g., in the clinic as a diagnostic tool for diabetes and in the food industry. The Glucose concentration in the blood is a crucial sign in various health conditions like diabetes and several metabolic dysfunctions. Because diabetic patients must carefully control their blood glucose level, the blood glucose self-monitoring for measuring sugar levels in clinics and at home or the workplace is significantly needed. It reported that Glucose biosensors show superlative stability, strong sensitivity, and limited response time (e.g., 10s) for glucose measurements because the electrons are migrated straightaway from the electrode facet to the substrate molecule via the active site of immobilized GOx, or vice versa [69, 70]. Commonly a GOx electrode is fabricated by decomposing GOx in phosphate-buffered saline (PBS) to the electrode surface following by its coating with Nafion to avoid enzyme leaking and remove foreign interferences. Glucose sensing guides by catalytic interaction between glucose and oxygen on the working electrode, which produces gluconic acid and hydrogen peroxide ($H_2O_2$), then $H_2O_2$ electrochemically reduces to hydrogen, and the electro-oxidation current detects after applying of appropriate potential to the system [58, 71, 72]. As the enzyme immobilization on the electrode facet significantly affects by the architecture of nanostructures, different morphology of ZnO nanomaterial has been utilized to fabricate glucose biosensors [69,73, 74].

Liu et al. produced a glucose biosensor using ZnO nanorod film grown on indium tin oxide (ITO). Glucose was shown to respond linearly from 5 to 300 µM, and the biosensor measured a limit of detection of 3 µM [75]. In a study by Umar et al., highly dense and well crystallized ZnO nanonails were utilized to fabricate an efficient glucose biosensor. According to their results, elevated sensitivity of 24.613 µA $mM^{-1}$ $cm^{-2}$ with a response time <10 s and a limit of detection of 5 µM were observed [70]. The carbon decorated ZnO nanowire arrays generate a straight electron path to promote electron movement from the enzyme to electrode surface with the high conductivity of carbon which makes it an appropriate material for direct electrochemistry of enzymes and mediator-free enzymatic biosensors. In research conducted by Liu et al., a highly sensitive glucose biosensor contingent on these nanostructures was fabricated with a significant low of a detection limit (1 µM) [76]. It is shown that ZnO nanoparticles enhance the electrical conductivity of the enzyme electrode by increasing the motion of electron movement between the active site of GOx and the electrode surface and considerably enhancing the current signal in comparison to the electrode without ZnO nanoparticles [77].

To highlight the impact of ZnO nanoparticles dimensions on the capability of direct electron transfer, Aini et al. [78] synthesized a glucose biosensor utilizing ZnO nanoparticles, eggshell membrane, and ionic liquid onto a glassy carbon electrode. An enhancement in the consignment boundary for enzyme immobilization and ease the interaction between (GOx) and the electrode were observed. Moreover, ZnO nanoparticles were fabricated using graphene-carbon nanotubes (CNTs) hybrid to create an enzyme-based glucose biosensor. A large linear scale (10 µM-6.5 mM) of glucose in the biosensor and a limit of detection of 4.5 µM were shown [79]. In another group, the electrochemistry of GOx was investigated via using graphite nanosheets and ZnO nanoparticles, that were electrochemically grown on a screen-printed electrode. Linear response range to glucose (0.3 to 4.5 mM) and a limit of detection of 0.07 mM were reported [80]. Another study was carried out to address how the highly aspect ratio and well-ordered ZnO nanorods formed on a Si/Ag electrode can influence the GOX immobilization and the biosensors sensitivity. Based on its results, superior sensitivity of 110.76 µA$mM^{-1}$ $cm^{-2}$, broad linear performance scale of 0.01–23.0 mM, and a fast response time of < 1 s were obtained. The good consequences of such a review were associated to the larger number of enzymes immobilized on the high aspect ratio ZnO nanorods [81].

Beside a higher aspect ratio of ZnO, it was reported that densely packed ZnO arrays are more efficient to fabricate highly performed glucose biosensors [82]. As shown in Fig. 5, the glucose sensitivity estimations were significantly affected by the density of surface areas, as the measured sensitivity of low, medium, and high density ZnO were 16.5, 41.3, and 69.8 nA/ (µM $cm^2$), respectively. Asif et al. [58, 83] developed a selective electrochemical sensor for intracellular estimations of glucose by using ZnO-nanorods. The nanorods were synthesized on the tip of a silver-coated borosilicate glass capillary (0.7 µm diameter) employing an aqueous chemical deposition approach and then coated with GOx. Moreover, the probe was utilized to particularly identify the intracellular level of glucose in two sorts of human adipocytes (fat cells) and frog oocytes (egg cells) cells. According to these measurements, a rapid response time to glucose (< 1 s) with a linear potential difference over the expected concentration scale of interest (0.5-1000 µM) were observed. Kong et al. applied a two-step crosslinking method to develop a glucose biosensor, in which ZnO nanorods were electrochemically deposited on the Au substrate then were chemically etched to fabricate ZnO nanotube arrays. The biosensor exhibited a broad linear response for glucose within 50 µM to 12 mM [84].

Hierarchical compositions have been fabricated by growing smaller morphology of nanomaterials on the primary ZnO nanostructures to increase the surface-to-volume ratio [85,86,87]. In a study conducted by Miao et al., ZnO nanowires deposited on silicon nanowires by a thermal decomposition method, then GOx immobilized on ZnO/Si hierarchical nanowire composite to develop a glucose biosensor [86]. Superior sensitivity of 129 µA$mM^{-1}cm^{-2}$ and a low limit of detection of 12 µM, and better durability and accuracy, were shown.

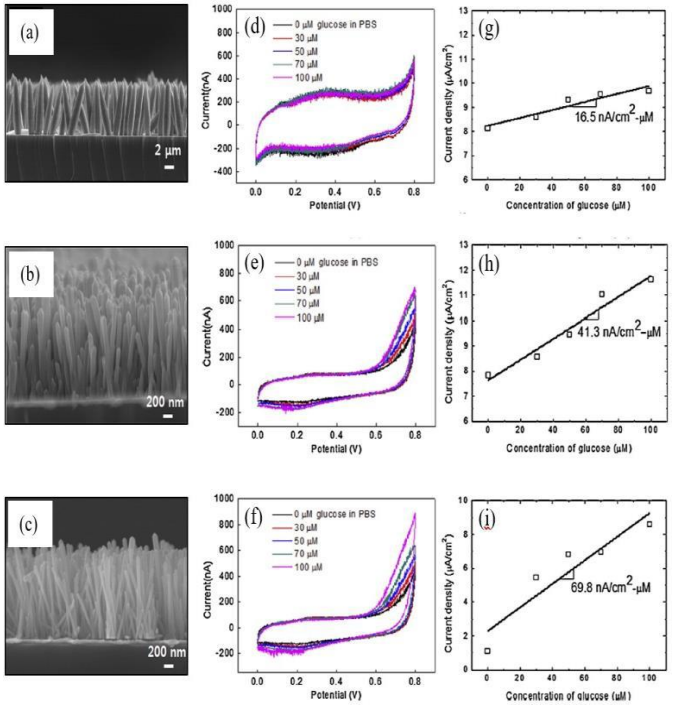


**Figure. 5:** FE-SEM photograph of 1D ZnO (a) ZnO-a (Length 7.7 _m; Diameter 1.5 _m); (b) ZnO-b (Length 1.58 _m; Diameter 0.105 _m); and (c) ZnO-b (Length 1.4 _m; Diameter 0.06 _m). Cyclic voltammograms of the 1D ZnO based glucose sensor (d) ZnO-a; (e)

ZnO-b; and (f) ZnO-c. The current density versus glucose concentration (g) ZnO-a; (h) ZnO-b; and (i) ZnO-c [82].

In addition, 3D hierarchical nanostructures have integrated with the p-n junction interface to boost the biosensing efficiency, as the electric field at this interface improves migrating an electron from the analyst to the electrode. Fan et al., [88] used $Co_3O_4$ as *n*-type semiconductors and ZnO as *p-type* to build *p-n* junctions by decorating ZnO nanofibers with $Co_3O_4$ nanoparticles, as demonstrated in Fig. 6. Introducing GOx/$Co_3O_4$/ZnO working electrode in the sensor, leading to an elevated sensitivity of 116.64 µA $mM^{-1}cm^{-2}$ compared to sensors with GOx/$Co_3O_4$ and GOx/ZnO functionalized electrodes (47.55 and 40.57 µA $mM^{-1}$ $cm^{-2}$, respectively).

Furthermore, considerable studies have been carried out to investigate the influence of ZnO/metal nanocomposites on the glucose-sensing process [89, 90, 91]. It reported that gold nanoparticles could serve as a conduction centre to promote transferring electrons among the redox centre of GOx and the electrode and boost the enzymatic activity of GOx [92, 93]. In research conducted by Tian et al., [90] working electrode of (ITO)/ZnO/Au/GOx) was synthesized via depositing a plant-like ZnO nanostructure on an ITO coated glass substrate, then ZnO nanostructure was patterned using Au nanoparticles of 23 nm diameter. The measured sensitivity of the sensor was 3.12 µA$mM^{-1}cm^{-2}$ in the linear scale of 50–400 mg/dL. Another group utilized a solution-based deposition approach, Au nanocrystals, and ZnO nanorods to produce ZnO nanorods/Au hybrid nanocomposites. The modified working electrode was built as ZnO/Au//GOx/Nafion. Based on its result, the sensor displayed a superlative sensitivity of 1492 µA $mM^{-1}$ $cm^{-2}$ over the concentration scale of 0.1-33.0 µ [91]. Linxia et al. [89] exploited the broad surface area of 3D ZnO, which led to efficient adsorption capacity, and the catalytical activity of Au nanoparticles to produce hybrid nanostructures, which was employed with a modified glass carbon electrode. The glucose biosensor showed a limit of detection of 0.02 mM in a large linear scale (1 – 20 mM).

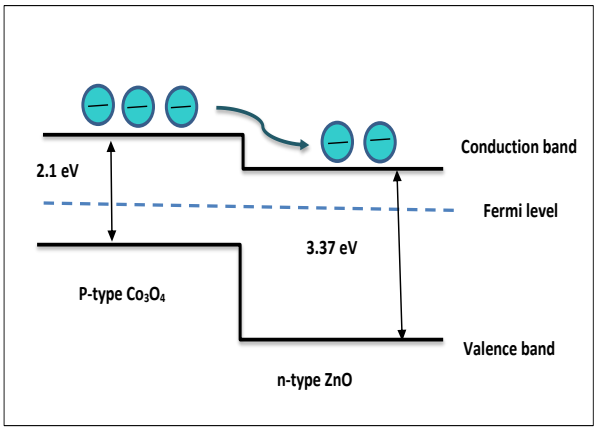


**Figure. 6:** Diagram of the $Co_3O_4$/ZnO p-n junction [88].

Although the commercial enzymatic biosensors of the GOx enzyme have been highly demanded on the market, they experience several weaknesses include lack of long-term stability and less reproducibility. Additionally, GOx is affected by some environmental conditions, e.g., temperature, pH, and chemical structure of a biological medium. Besides the enzymatic degradation over a long term which in turn causing a decrease in sensitivity is another obstacle when the enzymatic sensor is implanted into the human body [94]. To overcome those challenges, a considerable effort is dedicated to accomplishing highly sensitive enzyme-free glucose biosensors. Typically, the non-enzymatic sensors work according to the immediate oxidation of glucose on a modified working electrode surface with an inorganic electrocatalyst material. The detection procedure shows in Fig. 7a [95]. First, the depletion area of the primary channel that comprises ZnO nanoparticles and its current. When the PBS inserts into the system, the depletion layer within these nanoparticles reduces due to the positively charged ions of PBS on the channel facet (Fig. 7b) subsequently, the transferred current in the channel escalated. Once the channel exposes to the targeted sample, the depletion area is broadened (Fig. 7c) because of freed electrons generated by glucose. Therefore, the amount of the current of the primary channel is in proportion to the number of molecules of glucose, as the glucose concentration is varying inversely to the current value.

Despite ZnO suffers from the low sensing capacity of glucose [96, 97, 98], the combination of nanocatalyst with ZnO nanostructures leads to generate 3D hierarchical nanostructures, which produce a wide surface area for superlative catalytic activity and effective electron transport, leading to enhancing sensing procedure. Many catalyst components have been employed for preparing enzyme-free glucose sensors using ZnO nanomaterials, such as noble catalysts and their compounds, and CNTs (see Table (1)). Park et al. deposited ZnO nanoparticles on a plastic substrate to produce enzyme-free glucose biosensors for the first time [95]. However, some catalytic species are less efficient e.g., Pt was reported to degrade with some elements presented in human serum. Additionally, Au electrodes restrict because of their risk of chloride poisoning and low chemisorption of glucose [99]. However, some low-priced transition metals e.g., Co, Cu, and Ni are much applicable and have no chloride poisoning effect.

It was reported by Zhou et al. that ZnO hybrids of Pt, Ni, and Co nanoparticles and doped Au, C, and Al metals enhanced the catalysis interaction and conductivity of ZnO based glucose biosensor [**100**]. However, the electron transfer capability was poor causing some electrons to return to the GOx efficient site. Therefore, Zhou et al. [**100**] boosted the electron transferring by doping Ag, and the sensor showed 85 µA/(mM_$cm^2$) of sensitivity and 1.5 µM of a limit of detection. Moreover, in another conducted study [101], the sensitivity and catalytic activity to glucose detection were enhanced by doping Copper as the electrochemical characteristics of free enzyme glucose sensors enhanced due to the generation of several electro-active points.

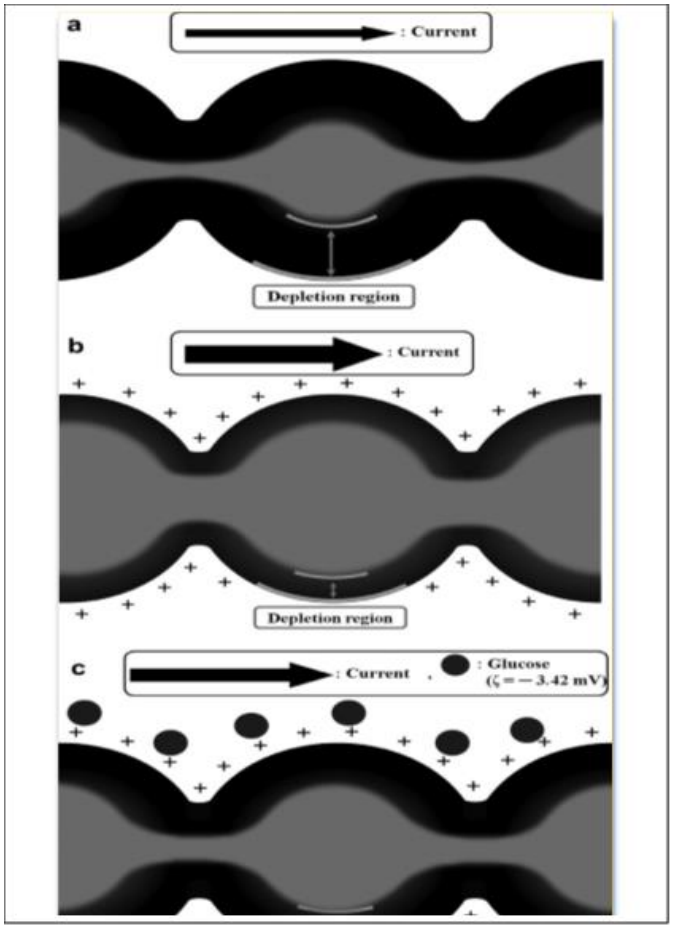


**Figure. 7:** the sensing process of glucose level by ZnO nanoparticles

(a) the primary channel of ZnO nanoparticles, (b) a decrease of the depletion area of the ZnO nanoparticles channel, (c) an expansion of the depletion area of the ZnO nanoparticles channel [100].

Most importantly, enzyme-based glucose sensors stand on the selective catalytic efficacy of the oxidation reaction of a target analyte, which in turn result to enhancing selectivity to different intrusive particles. Hence, it is critical to comprehend the mechanism of the selectivity of ZnO-based sensors without the existence of the enzyme. It was reported that ZnO-CuO, ZnO-NiO, and ZnO-Ni $(OH)_2$-modified electrodes showed reasonable selectivity to various electroactive molecules, including ascorbic acid, L-aspartic acid, dopamine, and uric acid [102, 103, 104, 105] thus, the sensor selectivity is guided by electrostatic repulsion interaction. It is worth noting that, in selectivity analysis of the nonenzymatic biosensors, the percent of glucose to intrusive molecules is mostly 10: 1, taking into account that the blood glucose level is at least 30 times larger than those of the intrusive particles [104, 106, 107]. Therefore, one disadvantage of the enzyme-free sensors is its dependency on the expectation of a small concentration of the intrusive particles in the blood instead of catalytic activity to glucose. Another downside of these sensors is that they operate only in basic conditions as the reaction of glucose detection include OH– anions therefore, human blood should be diluted with main electrolytes for the glucose estimations [108].

**Table 1. Various electrodes employed in the production of glucose biosensors using ZnO nanostructures.**

| Electrode | Sensitivity | Linear range | Detection limit | Response time | Ref. |
|---|---|---|---|---|---|
| Nafion/GOx/ZnO nanorods/Ag/Si substrate | 110.76 µA $mM^{-1}cm^{-2}$ | 0.01–23.0 mM | 0.1 µM | < 1 s | 89 |
| Single ZnO nanofiber on Au electrode | 70.2 µA $mM^{-1}cm^{-2}$ | 0.25–19 mM | 1.0 µM | ~4 s | 74 |
| Nafion/GOx/ZnO nanowires /Si nanowires/Si wafer | 129 µA $mM^{-1}cm^{-2}$ | 0.2–20 mM | 12 µM | | 86 |
| EGFET based on Al-doped ZnO nanostructures | 60.5 µA $mM^{-1}cm^{-2}$ | 0–13.9 mM | | | 171 |
| Nafion/GOx/ZnO nanotubes /ITO/glass | 30. 89 µA $mM^{-1}cm^{-2}$ | 10µM–4.2mM | 10 µM | <6 s | 175 |
| Nafion/GOx/Au NPs/plant-like ZnO/ITO/glass | 3.12 µA $mM^{-1}cm^{-2}$ | 50–400 mg/dL | | | 90 |
| GOx/Au NPs/3D hierarchical ZnO nanostructures/GCE | 1.409 µA $mM^{-1}cm^{-2}$ | 1–20 mM | 20 µM | | 89 |
| Nafion/GOx/Au nanocrystals/ZnO nanorods/GCE | 1492 µA $mM^{-1}cm^{-2}$ | 0.1–33.0 µM | 10 nM | 5 s | 91 |
| Chitosan/GOx/$Co_3O_4$-ZnO nanostructures/GCE | 116.64 µA $mM^{-1}cm^{-2}$ | 0.01–5 mM | 1.38 µM | 4 s | 88 |
| GOx/ZnO nanorods/borosilicate glass capillary | 42.5mV/ decade | 500 nM–1 mM | | < 1 s | 58 |
| $Zn_{0.90}Co_{0.10}O$ nanoparticles/GCE | | | 5 µM | <4 s | 98 |
| ZnO/MWCNTs/GCE | 64.29 µA $mM^{-1}cm^{-2}$ | 1–10 mM | 0.82 mM | | 176 |
| $Ni(OH)_2$ nanorods/ZnO nanorods/ITO | 1569 µA $mM^{-1}cm^{-2}$ | 2–3862 µM | 0.6µM | | 102 |
| Ni nanoparticles/ ZnO Hexagonal prisms/GCE | 824.34 µA $mM^{-1}cm^{-2}$ | 1 µM–8.1 mM | 0.28 µM | 4 s | 177 |
| $Ni(OH)_2$ nanoflakes/ZnO nanorods/ITO | 1.85 mA $mM^{-1}cm^{-2}$ | 0.04–2.10 mM | | <1 s | 103 |
| NiO/ZnO mesoporous composite/GCE | 120.5 µA $mM^{-1}cm^{-2}$ | 0.5 µM–6.4mM | 0.5 µM | <3 s | 178 |
| ZnO–CuO hierarchical nanocomposites/FTO/glass | 3066.4 µA $mM^{-1}cm^{-2}$ | 0.47µM–1.6mM | 0.21 µM | | 104 |
| ZnO–CuO porous spheres coreshell structure composite with/GCE | 1,217.4 µA $mM^{-1}cm^{-2}$ | 0.02–4.86 mM | 1.677 µM | <2 s | `179 |
| ZnO nanorods/CuO nanoleafs/Cu substrate | 408 µA $mM^{-1}cm^{-2}$ | 0.1–1 mM | 18 µM | | 106 |
| CuO-ZnO composite nanofibers/Pt | 463.7 µA $mM^{-1}cm^{-2}$ | $8\times10^{-7}$–3.88 $\times10^{-3}$ M | 0.126 µM | | 107 |
| CuO nanoflowers/ZnO nanorods/brass substrate | 1362.7 µA $mM^{-1}cm^{-2}$ | | 1 µM | 5s | 180 |
| Nafion/ZnO-GOD/Nafion/GC | 23.4 µA /mM $cm^2$ | | 10 µM | 7 s | 181 |
| Nafion/GOx/ZnO NRs/ITO | 48.75 µA/m M | 0.05 – 1 mM | | 10 s | 182 |
| Au-ZnO/rGO/ITO | 10.93 $\mu AmM^{-1}cm^{-2}$ | | 0.2 µM | | 203 |
| Nafion/GOx/ZnONRs/Au/PET | 5.40 µA m $M^{-1}cm^{-2}$ | 0.1mM –12 mM | 17.8 µM | | 204 |

### 4. 2. ZnO Nanostructures based cholesterol biosensors

The optimal cholesterol content in the human being is below 5.2 mM, as abnormal blood cholesterol levels are related to different diseases, including heart and blood vessel diseases, coronary artery disease, cerebral thrombosis, arteriosclerosis, lipid metabolism disorders [109]. Therefore, monitoring the cholesterol amount in the blood is essential for healthcare purposes. In the state of cholesterol sensing, cholesterol oxidase (ChOx) catalyzes the reaction between cholesterol and oxygen to form hydrogen peroxide. To fabricate cholesterol biosensors, several ZnO nanostructures, such as nanoparticles [110], nanospheres, [111] nanowalls, [112] nanotubes, [113] and nanorods, [114, 115] have been employed (see Table (2)).

It reported that applying ZnO nanoparticles as nanohybrid structures with carbon nanotube (CNT) might be a suitable substitute for natural enzymes [116]. According to its findings, the combination of the catalytical efficiency of ZnO and CNT leading to a high catalytic response [116]. Another process demonstrated to develop a cholesterol biosensor via employing ZnO nanoparticles as the link between enzyme and electrode without combining it to different nanostructures [110]. The broad exposed surface of these nanoparticles provides a strong adsorption capability of Chox, increasing the enzyme bonding capacity on its surface and assisting electrons to migrate among the effective points of functionalized Chox and the modified electrode [110]. Hence, better performance and a less limit of detection of the biosensor were observed. A similar study carried out by Vilian et al. [117] reported that ZnO nanoparticles offer a direct electron transport pathway between the enzyme and the electrode surface, thus effective sensing performance can be achieved.

A potentiometric biosensor was prepared by applying ZnO nanowalls encapsulated and a ChOx-containing lipid membrane [112] (Fig. 8a, b). Owing to the large surface-to-volume area of ZnO nanowalls, positive and negative layers along their nonpolar planes were generated, thus the absorption activity of ChOx was enhanced. According to cholesterol estimation of the designed biosensor, superior selectivity of different analytes include maltodextrin, dextrose, ascorbic acid, lactose, sorbitol, glucose, leucine, etc., was shown. The distinctive sensing properties of ZnO nanowall are linked to its wide surface area and efficient electric conduction. The biosensor sensitivity was reported to escalate from 32 mV/decade to 57 mV/decade with a rapid response time of 5 s. Furthermore, the reliability of these device was tested by measuring cholesterol levels in diluted blood serum specimens, and the measurements were in reasonable agreement with the clinical biochemistry measurements [112].

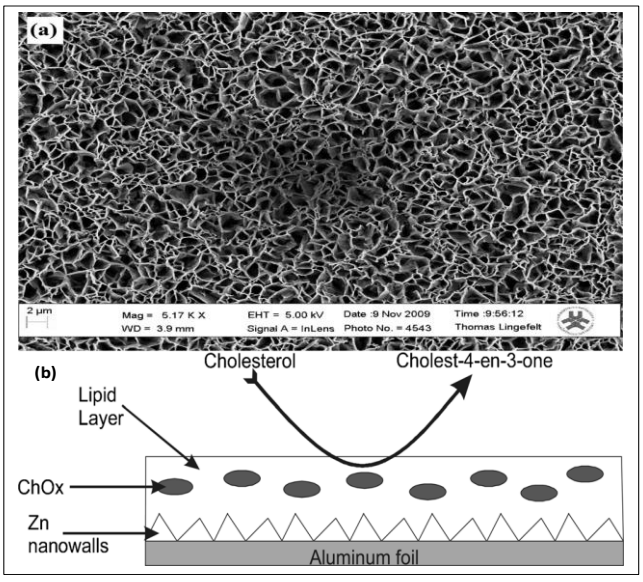


**Figure. 8:** (a) SEM photograph of ZnO nanowalls; (b) Demonstration of the biosensor design [112].

In another study, an extremely sensitive cholesterol biosensor was synthesized using platinum-incorporated fullerene-like ZnO hybrid nanospheres onto a glassy carbon electrode [111]. The designed biosensor showed a sensitivity of 1886.4 mA/ (M $cm^2$) in a linear operation scale from 0.5 to 15 µM and a limit of detection less than 0.2 µM**.** A highly selective determination of cholesterol has been obtained by applying ZnO and platinum nanoparticles to build Pt/Au hybrid ZnO nanorods [114]. Acceptable findings were observed by employing the sensor to estimate cholesterol in diluted blood serum specimens. Additionally, the sensor had 0.03 µM of a limit of detection and superior selectivity for ascorbic acid, uric acid, and L-cystine.

**Table 2. Various electrodes employed in the production of cholesterol biosensors using ZnO nanomaterials.**

| Electrode | Sensitivity | Linear range | Detection limit | Response time | Ref. |
|---|---|---|---|---|---|
| Stabilized lipid film/ChOx/ZnO nanowalls/Al foil | 57 mV/ decade | $10^{-6}$–$10^{-3}$M | $4\times10^{-7}$ | ~5 s | 112 |
| Nafion/ChOx/Ptincorporated fullerene-like ZnO nanospheres/GCE | 1886 mA/$M^{-1}cm^{-2}$ | 0.5–15 µM | <0.2 µM | <5 s | 111 |
| Nafion/ChOx/ZnO nanorods/Ag/Si substrate | 74.1 µA $mM^{-1}cm^{-2}$ | 0.01–16.0 mM | 0.0015 µM | <2 s | 118 |
| Nafion/ ChOx/Pt-Au functionalized ZnO nanorods/chitosan-MWCNTs/GCE | 26.8 µA $mM^{-1}cm^{-2}$ | 0.1–759.3µM | 0.03µM | <6 s | 114 |
| Nafion/ChOx/ZnO nanoparticles/Au | 23.7 µA $mM^{-1}cm^{-2}$ | 1.0–500 nM | 0.37 nM | < 5 s | 110 |
| Nafion/ChOx/ZnO nanorods/Au | 61.7 µA $\mu M^{-1}$ $cm^{-2}$ | 1.0–15.0 µM | 0.012 µM | <5 s | 115 |
| ChOx/nano-ZnO/ITO | 0.059µA/mg $dl^{-1}$ $cm^{-2}$ | 5–400 mg/dl | 0.5 mg/dl | 10 s | 121 |
| ChOx/nano-structured ZnO/Pt/Si | 153 µA $mM^{-1}cm^{-2}$ | 0.12–12.93mM | | 5 s | 119 |
| ChEt–ChOx/ZnO/Pt/Si | 117 µA $mM^{-1}cm^{-2}$ | 0.5–12 mM | | | 120 |
| ChOx/ZnO nanocrystals/Ag nanowires/graphene oxide- chitosan/ITO | 9.2 µA $\mu M^{-1}$ $cm^{-2}$ | 6.5 µM–10mM | 0.287 µM | | 122 |
| Nafion/ChOx/ZnO nanotubes/Ag/Si | 79.40 µA $mM^{-1}cm^{-2}$ | 1 µM–12 mM | 0.5 nM | ~2 s | 113 |
| ChOx/ZnO-ZnS nano-heterostructure/chitosan/GCE | 293 mA $M^{-1}cm^{-2}$ | 0.4–2 mM | 0.08 mM | <5 s | 123 |
| ChOx/ chitosan/ZnO-ZnS microtubes/GCE | 52.67 µA $mM^{-1}cm^{-2}$ | 0.4–3.0 mM | 0.02 mM | <5 s | 124 |
| ChOx/ZnO nanorods/Ag | 35.2 mV/ decade | $1\times10^{-6}$ – $1\times10^{-2}$ M | | 10 s | 183 |
| ChOx/ZnO/ITO/glass | 57.533µAm $M^{-1}cm^{-2}$ | 25 – 500 mg/dl | | | 184 |
| ChOx/ ZnO nanorods modified with $Fe_2O_3$ nanoparticles | 37.34 µA $mM^{-1}cm^{-2}$ | 0.1 – 60.0 mM | | | 205 |

As we mentioned earlier in the case of glucose detection, the high aspect ratio of ZnO plays an essential role in the efficiency of cholesterol biosensors. It was reported that a larger amount of immobilized ChOx and improved electron conduction leading to a significantly sensitive biosensor based on ZnO nanorods/ Ag [118], as showed in Fig.9. In other studies, the vapour phase transport deposition approach was applied to synthesize ZnO nanolayers on Pt-coated Si substrate to immobilized ChOx [119, 120] and cholesterol esterase (ChEt) [120]. excellent sensitivities of (153 µA/ (mM $cm^2$) [119] and 117 µA/ (mM $cm^2$) [120] were shown contingent on the modified working electrodes ChOx/ZnO/Pt/Si and ChEt-ChOx)/ZnO/Pt/Si, respectively. Furthermore, the sol-gel synthesis technique was utilized to manufacture ZnO nanostructured films on ITO substrate to develop cholesterol biosensors [121]. According to its findings, superior sensitivity of 59 nA/ (mg dL $cm^2$) and a short limit of detection of 0.5 mg/Dl within a large linearity scale of 5.0–400 mg/dL were showed.

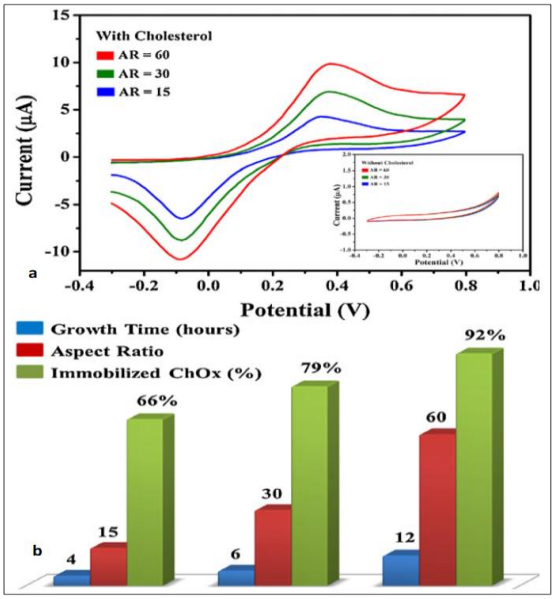


**Figure. 9:** (a) Cyclic voltammetry analysis for the aspect-ratio dependency of biosensors without (insert) and with 2 mM cholesterol in 0.1 M PBS (pH 7.4) at scan rate of 100 mV/s; (b) bar charts displaying the connection among the enzyme immobilization percent and the ZnO NRs aspect ratio with growth time [118].

Wu et al. [122] also prepared an extremely sensitive and selective cholesterol biosensor by ChOx immobilization on ZnO/Ag/graphene oxide-chitosan/ITO working electrode. ZnO nanocrystals assisted in immobilizing ChOx (IEP ~ 5.0) through intensive electrostatic interaction, while Ag nanowires expedited to catalyze $H_2O_2$ reduction reaction. The sensor displayed an improved sensitivity of 9.2 µA $\mu M^{-1}cm^{-2}$ within a linearity scale of (6.5-10 mM). The modified electrode also exhibited better stability and high selectivity to glucose, oxalic acid, citric acid, L-cysteine, and ascorbic acid. Giri et al. [123, 124] tried to boost the sensing activity by utilizing ZnS-ZnO heterostructures, as the electric field at the ZnS/ZnO interface was assumed to promote electron transfer rate, resulting in increasing sensor efficiency. According to the sensing mechanism of ChOx/ZnSZnO heterostructure-modified electrodes, the conduction band of ZnS exists higher than that of ZnO, therefore electrons freed by ChOx are migrated to the exterior ZnS by the $Fe^{2+}/Fe^{3+}$ redox pair, and the electric field at the ZnS/ZnO interface expedites electrons traveling to the electrode (Fig. 10). A systematic study conducted by Umar et al. [115] investigated the influence of pH concentration on the efficiency of cholesterol biosensors fabricated using ZnO nanostructures. It reported that the highest current output occurs in the pH region of 6.8–7.6 and the minimums on either side of this pH region. This observation was associated to the pH impact on the enzyme connection for its substrate**.**

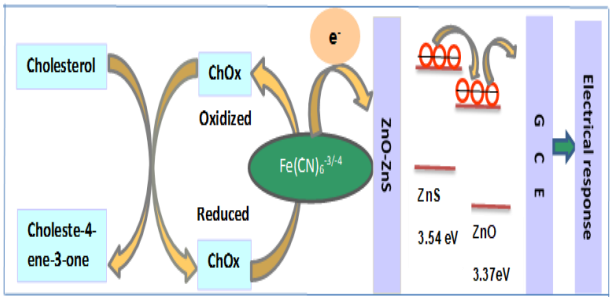


**Figure. 10:** Representation of the detection procedure of the ZnO-ZnS microtube-based electrode [124].

### 4. 3. ZnO Nanostructures based L-lactic acid biosensors

Lactate acid concentrations have been employed as an important medical diagnostic tool, assessing patient health conditions and study diseases. A high amount of lactic acid in blood induces several health issues namely, shock, heart failure, chronic kidney disease, respiratory insufficiency, chronic renal failure, and metabolic disorders [125]. Lactate is an essential metabolite that human cells can use as fuel, specifically through an intensive workout. Once the required energy for tissues is inadequate by aerobic respiration, lactate levels increase by the anaerobic metabolism. Generally speaking, the liver and kidney are responsible for sufficiently clear the accumulated concentration of lactic acid which, can develop lactic acidosis. Therefore, the production and consumption of lactate are extremely ruled by lactate homeostasis in a healthy human being. Lactic acidosis can cause by two types of disorders. The first type involves a reduction in tissue oxygenation including, shock, left ventricular failure, septicemia and poisoning with carbon monoxide and cyanide. The other type of diseases can develop by certain drugs or toxins with systemic disorders, including failure of a renal and hepatic system, diabetes and malignancy or inborn error metabolism [126]. Therefore, blood lactate levels as alarm signals help in the diagnosis and treatments for many diseases and severe illnesses.

In addition, lactate plays a key role in sports medicine, particularly for testing athletics physical fitness. During exercise, the blood lactate level acts as an index for the athletic performing condition and fitness as high lactate levels generate a low level of pH in the blood which, causing fatigue. Furthermore, lactate has a key function in the food and fermentation production. Lactate produces from many

fermentative items e.g., fermented dairy products, wine, cured meat and fish and pickled vegetables, therefore lactate reacts as an indicator for the freshness and quality of processing food [127]. Several enzymes have been used for L-lactic acid detection and biosensor manufacture. The most used ones are lactate dehydrogenase (LDH), cytochrome b2, lactate monooxygenase, and lactate oxidase (LOD). Once negatively charged LOD is immobilized L-lactic acid oxidizes with producing of unsteady pyruvic acid, which directly decays into pyruvate and Hydrogen peroxide, which reduces to $H^+$. Different nanomaterials are widely applied to develop lactate biosensors include ZnO nanostructures, carbon nanotubes, and Au nanoparticles. In particular, ZnO nanostructure is a fascinating platform for lactic acid biosensor manufacturing [128, 129, 130]. The LOD layer was coated with polydiallyldimethyl ammonium chloride (PDDA) and immobilized on ZnO nanoparticles grown on multi-walled carbon nanotubes (MWCNTs) [131]. A sandwich-like layered composition of the PDDA/LOD/ZnO/MWCNTs cathode offered a suitable biological micro-surrounding to maintain the enzyme efficiency and limit leakage of the LOD molecules. Lactic acid biosensor had a sensitivity of 7.3 µM/mM, a limit of detection of 6 µM, and excellent durability and selectivity (see Table (3)).

**Table 3. Various electrodes employed in the fabrication of lactic acid biosensors using ZnO nanostructures.**

| Electrode | Sensitivity | Linear range | Detection limit | Response time | Ref. |
|---|---|---|---|---|---|
| PDDA/LOD/ZnO nanoparticles/MWCNTs | 7.3µMmM$^{-1}$ | 0.2–2.0 mM | 6 µM | 6 s | 131 |
| Nafion/LOD/ZnO nanotetrapods/Au | 28.0 µA mM$^{-1}$ cm$^{-2}$ | 0.0036 –0.6 mM | 1.2 µM | 10 s | 129 |
| LOD/ZnO nanorods/Au/glass | 41.33 mV/decade | $10^{-4}$ – 1 mM | $1 \times 10^{-4}$ mM | <10 s | 128 |
| LOD/In-doped ZnO nanowires-gated AlGaAs/GaAs HFET | | 3 pM–3 mM | 3 pM | 1 s | 185 |
| Nafion/LOD/ ZnO nanowires/Au | 15.6 µA mM$^{-1}$ cm$^{-2}$ | 12 µM–1.2 mM | 12 µM | | 186 |
| PET/Au/ZnO nanoflakes/ LOx | 2.23 µA/M /cm$^2$ | 10 pM-10 µM | 10 pM | | 187 |
| PET/ ZnO nanoflakes/ LOx | 11.76 µA/decade/cm$^2$ | 10 pM-20 mM | 1.26 nM | | 206 |
| FePt NPs/CZO film | 25.32 mV/mM | | | 16 s | 207 |

In contrast to a biosensor synthesized via employing Pt electrodes functionalized with LOD-glutaraldehyde-bovine serum albumin (BSA), the thermal stability of LOD immobilized on ZnO nanoparticles was investigated within the temperature scale of (10 - 50°C). The biosensor performance of the PDDA/LOD/ZnO/MWCNT electrode showed an Arrhenius temperature dependence through a continual increase with temperature, whilst the output signal of the LOD–glutaraldehyde–BSA biosensor decreased considerably at temperatures over 40°C. The excellent thermal resistivity of the PDDA/LOD/ZnO/MWCNT sensor was associated with the unique multilayer composition of ZnO nanoparticles which, offered a suitable design for the LOD loading [131].

It was reported that the broad surface area of ZnO nanorods with a high isoelectric point help in easily immobilizing enzyme to the surface and promoting direct electron pathway among the active points of the LDH and the electrode surface. Nesakumar et al. [132] immobilized LDH enzyme with chitosan onto the ZnO nanorods to develop a lactic acid biosensor. The modified electrode Au/ZnO/LDH showed a limit of detection of 4.73 nmolL$^{-1}$ and sensitivity of 1.832 µ A µmol$^{-1}$ L within a response time of less than 1s. In a study carried out by Lei et al. [129], 3D ZnO nanotetrapods was employed for preparing L-lactic acid biosensors. After testing in PBS, the modified electrode Nafion/LOD/ZnO nanotetrapods/ Au exhibited a sensitivity of 28.0 µA mM$^{-1}$ cm$^{-2}$, a limit of detection of 1.2 µM, and a linear response range of 3.6 µM–0.6 mM. sensitivity is an essential aspect to develop highly performed lactate biosensors, different elements can hugely affect the rate of biosensor sensitivity.

Typically, sensitivity is a proficiency of the physical design of the electrode and the immobilized biomolecule, hence the electrode configuration can modify, e.g., by increasing its surface area to loading large amounts of the enzyme which, result in producing highly sensitive enzymatic biosensors. To optimize the sensing process, reducing the biosensor dimension to the micro or nanoscale is highly required, which might strengthen the binding interactions of biomolecules and generate a lower detection limit. Biosensor produced by immobilizing the LOD enzyme on the ZnO nanorods combining with glutaraldehyde as a crosslinker for LOD was established by Ibupoto et al. [128]. The Au/ZnO/LOD bioelectrode showed a significant sensitivity of 41.33±1.58 mV decade$^{-1}$ and linearity over 0.1–1 mmolL$^{-1}$ with a fast time of 10 s.

### 4. 4. ZnO Nanostructures based uric acid biosensors

Uric acid is the final output of purine metabolism in the human body and can act as an antioxidant. The concentration of uric acid in human serum is between 25 to 75 mg/100 mL [133]. High amount of uric acid in the blood (hyperuricemia) or urine (hyperuricosuria) is a sign of various disorders [134]. Decreased uric acid levels link to multiple sclerosis and Parkinson disorders [135]. The first uric acid measurement was provided by Offer in 1894. According to his approach, the uric acid oxidizes to allantoin, which reduces phosphor tungstic acid to a tungsten blue chromophoric compound. However, such a technique has some drawbacks, e.g., interferences with other species that can produce the same interaction, which leads to poor selectivity [136]. Uricase enzyme was widely applied to sensitize the ZnO surface for uric acid detection (IEP ~ 4.3 or 4.6) [137, 138, 139, 140], which can immobilize on the ZnO surface. In the oxidation reaction, uricase catalyzes the uric acid to allantoin, $H_2O_2$ and $CO_2$. Then, allantoin receives a proton from water transforming into an allantoinium ion, which interacts with ZnO and develops potential difference at the electrode surface. Wang et al. fabricated a uric acid biosensor by using multiwalled carbon nanotubes (MWCNTs) and ZnO nanoparticles [138]. The ZnO-MWCNT-PG electrode was made by adjusting Pyrolytic graphite wafers (PG) with MWCNTs and then patterning ZnO nanoparticles onto the MWCNT surfaces. Lastly, uricase immobilized on the ZnO-MWCNT-PG electrode surface according to the isoelectric point variations of uricase and ZnO nanoparticles. The modified electrode was covered with 0.5% PDDA to remove probable impurities and inhibit the enzyme leaching.

A differential pulse voltammetry (DPV) was applied to estimate the interference impact of ascorbic acid, glucose, and L-cystine, and successfully all responses of those categories were isolated by the biosensor. A uric acid biosensor based on ZnO nanorods was produced in which nafion-modified glassy carbon electrode was decorated by ZnO nanorods and then uricase was electrostatically immobilized onto the electrode surface [141]. Elimination of the intervention of ascorbic acid, glucose and L-cystine was demonstrated. A uric acid biosensor based on ZnO nanowires was produced via Tzamtzis et al. [142]. Uricase was integrated with the lipid film before its polymerization on the ZnO nanowire surface, as the lipid film includes positively charged lipid ions which enhance the concentration of uric acid over the electrode resulting in intensifying the detecting and monitoring process. The biosensor displayed a small limit of detection, significant response time, and reasonable selectivity (see Table 4). The measured sensitivity of the lipid/ZnO biosensor (61 mV/decade) was twice as great as that reported in the absence of a lipid film (32 mV/decade).

A group of researchers assumed that non-aligned ZnO nanostructures-based biosensors might have poor performance because of the electrical discontinuity between the multinanowires [143]. Additionally, an individual ZnO nanowire-based biosensor would facilitate electron transportation to the electrode. So, according to a such assumption, a uric acid biosensor using a single ZnO nanowire was fabricated. The Nafion/uricase/ZnO wire/Au electrode was investigated in the PBS, and the sensor displayed a sensitivity of 89.74 µA mM$^{-1}$ cm$^{-2}$ in the linear scale (0.1 -0.59 mM) with reasonable selectivity and stability (see Table 4). However, the authors did not provide a comparative review about individual-wire based biosensors therefore, the conclusion on the outstanding efficiency of this structure was indecisive. As human serum and extracellular fluid of the central nervous system contain uric acid, ascorbic acid, and dopamine, it is extremely required to detect these components without cross-

interference. Therefore, enzyme-free biosensors fabricated using different nanocomposites have been utilized for sufficient identification of uric acid, ascorbic acid, and dopamine including, ZnO nanorods-Au NPs,[144] ZnO nanowires-graphene foam (GF),[145] reduced graphene oxide-ZnO, [146] carbon fibers-ZnO core-shell hybrids,[147] reduced graphene oxide-intercalated ZnO quantum dot nanoballs, [148].

It reported that ZnO nanostructures show a broad catalytic efficiency and offer a straightforward and rapid pathway for electron transport. Additionally, the porous design of the GF with a high surface area and active sites promotes the diffusion of electrolyte ions in the electrode and enhances the electric conductivity. High selective estimation of uric acid, dopamine, or ascorbic acid by a (DPV) using ZnO nanowires deposited on 3D GF was conducted by Yue et al. [145]. Based on DPV measurements, the current increases linearly with the analyte density as the ZnO/GF/ITO electrode showed the highest oxidation current. Conductive polymer-based nanocomposite structures are effective for the multi-analyte sensing, e.g., polypyrrole (PPy) and polyaniline (PANI) enable to make selective electrode that can identify differences among binding interactions, electrostatic interaction, or ion-exchange abilities [149, 150]. Besides, these nanocomposites have a wide surface area and high electrical conductivity, promoting electron movement in electrochemical reactions, consequently a significant enhancement in the biosensor sensitivity, selectivity, and limits of detection can be shown.

**Table 4. Various electrodes employed in the production of uric acid biosensors using ZnO nanostructures.**

| Electrode | Sensitivity | Linear range | Detection limit | Response time | Ref. |
|---|---|---|---|---|---|
| Nafion/Uricase/ZnO nanorods/Ag electrodes | 239.67 µA $cm^{-2}$ $mM^{-1}$ | 0.01–4.56 mM | 5 nM | ~3 s | 188 |
| Uricase/ZnO nanorods/GCE | | 5.0 ×$10^{-6}$ –1 × $10^{-3}$molL$^{-1}$ | 2.0 × $10^{-6}$ mol $L^{-1}$ | | 141 |
| Nafion/uricase/ZnO nanoflakes /Al/Au-coated plastic substrates | ~66mV/decade | 500 nM–1.5 mM | | 8 s | 189 |
| PDDA/uricase/ZnO NPs /MWNTs/pyrolytic graphite | 393 mA $cm^{-2}M^{-1}$ | 5 µM–1 mM | 2.0 mM | | 138 |
| Nafion/uricase/ZnO nanowires /Au-coated plastic substrates | 32 mV/decade | 1–1000 µM | | 6.25 s | 139 |
| Nafion/uricase/ZnO nanotetrapods/Au | 80 µA $mM^{-1}cm^{-2}$ | 0.8 µM–3.49mM | 0.8 µM | 9 s | 139 |
| Uricase-containing lipid film /ZnO nanowires/Au-coated plastic substrates | 61 mV/decade | 1.0–1000 µM | 0.4 µM | 6s | 142 |
| Nafion/uricase/ZnO wire/Au | 89.74 µA $mM^{-1}$ $cm^{-2}$ | 0.1–0.59 mM | 25.6 µM | | 143 |
| Nafion/Uricase/ZnO nanosheets/Ag/Si | 129.81 µA $mM^{-1}$ $cm^{-2}$ | 0.05–2.0 mM | 0.019 µM | 5 s | 190 |
| Uricase/single ZnO nanowire-based FET | | 1 pM–0.5 mM | 1 pM | several ms | 19 |
| Nafion/uricase/ZnO nanotetrapods-modified AlGaAs/GaAs HFET | | 0.2 nM–0.2 mM | 0.2 nM | ~1 s | 191 |
| ZnO/CuxO/ polypyrrole/GCE | | 0.5–70µM | 0.2 µM | | 151 |
| ZnO/PANI/reduced graphene oxide | | 100–1000 µM | 0.122 µM | | 149 |
| Au nanoparticles/ZnO nanorods/GCE | | 10–400 µM | 2.375 µM | | 144 |
| ZnO nanowires/graphene foam/ITO/glass | 4.24 µA $mM^{-1}$ $cm^{-2}$ | 0.1–60 µM | 1nM | | 145 |
| RGO–ZnO/GCE | | 3–330 µM | 1.08 µM | | 146 |
| Carbon fibers/ZnO core–shell hybrids | | 20–200 µM | 6.7 µM | | 147 |
| ZnO quantum dots/reduced graphene oxide sheets/ MWCNTs/Ni foam/GCE | 70.537 µA $mM^{-1}$ $cm^{-2}$ | up to 1.1 mM | 3.89 µA | | 148 |
| Nafion / ZnO QDs/ uricase | 4.0 µA/mMcm$^{-2}$ | 1 -10 mM | | | 192 |
| MZI coated with ZnO nanowires | 0.001 nm/ppm | 0-500 ppm | 5.74 % | | 193 |
| Nafion/uricase/ZnO NRs–ZnO NPs/FTO | 345.44 µA $mM^{-1}$ $cm^{-2}$ | 0.01–1.5 mM | 2.5 µM | | 208 |

Ghanbari and Hajheidari. [151] developed ZnO nanosheets/CuxO nanowires/PPy electrode to detect uric acid, ascorbic acid, and dopamine. To synthesize the modified electrode, CuxO nanowires and ZnO nanosheets were grown on a glassy carbon electrode using a solution-based technique. PPy nanofiber film as a conductive polymer with a well-aligned chain arrangement and wide surface-to-volume area allowing large adherence of the CuxO and ZnO and efficient charge movement**.** The ZnO/CuxO/PPy-modified electrode exhibited detection limits for ascorbic acid, dopamine, and uric acid of 25.0, 0.04, and 0.2 µM, respectively, which are in good agreement with the separate estimation for each component (25.0, 0.03, and 0.2 µM, respectively). Besides, it displayed acceptable reproducibility and selectivity against frequent intrusive elements, such as glucose, fructose, sucrose, lactose, cysteine, epinephrine, acetaminophen, serotonin, $K^+$, $Na^+$, $Ca^{2+}$, $Mg^{2+}$, $Zn^{2+}$, $NH4^+$, $Cl^-$, $NO_3^-$, $SO_4^{2-}$, and $HCO_3$. ZnO/ PANI /reduced graphene oxide nanocomposites were synthesized via an electrochemical deposition technique on a glassy carbon electrode to prepare simultaneously detective dopamine and uric acid biosensors [149]. Like the ZnO/CuxO/PPy-modified electrode, the ZnO/PANI/ reduced graphene oxide -based sensor displayed a superior sensitivity and selectivity for lower values of pH (4.0).

### 4. 5. ZnO Nanostructures based metal ion biosensors

Metal ions play essential roles in human health and the biological process by servicing as cofactors in enzymes, osmoregulatory, current carriers and also as factors in information processing and as integrators and stabilizers for proteins-lipids interaction [152, 153]. So, examining and regulating metal-ion concentrations in blood, interstitial fluid, and urine are important for physical and mental human health. The usual approach to identify metal-ion ratios utilizing ZnO nanomaterials includes a conformal coating of electrodes with ion-selective (ionophore-containing) monolayer-thin membranes based on polyvinyl chloride (PVC). The basic element of membrane-based ion-selective electrodes for a specific target ion is the ionophore (ion carrier), a component which selectively carries a specific metal ion over the membrane. An ion-selective biosensor was produced by Asif et al. [154] to measure intracellular $Ca^{2+}$ concentration in which an extended gate of a commercial metal oxide semiconductor field-effect transistor (MOSFET) was made based on ZnO nanorods. The sensing procedure to observe actual variations in $Ca^{2+}$ was performed using the electrochemical potential changes at the single-cell/ZnO nanorod interface. The extended-gate FETs (EGFETs) develops surface potential, which is combined with the gate potential, and hence the source-drain current relies upon the ion density in the sample solution. The ZnO nanorods were synthesized on the silver wire surface and coated with PVC membrane containing $Ca^{2+}$-specific ionophore (DB18C6). As illustrated in Fig. 11, the ZnO-nanorod electrode is extraneously linked at the gate terminal of a MOSFET in series. The interfacial potential differences on the ZnO electrode because of its interaction with $Ca^{2+}$ ions transformed into the drain current change of the MOSFET, and hence the $Ca^{2+}$ signal was amplified.

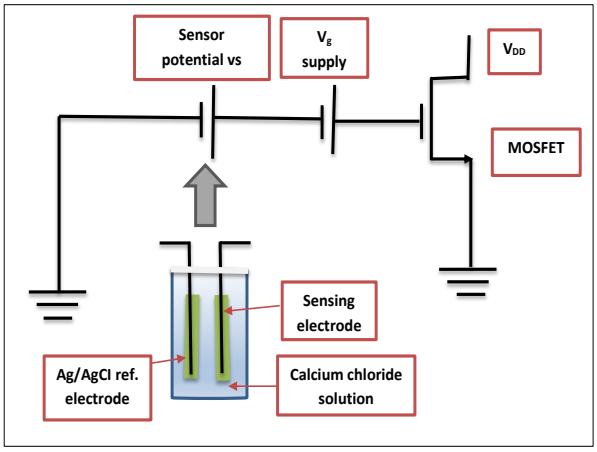


**Figure. 11:** A practical scheme for the $Ca^{2+}$ ion detection [155].

To intracellular monitoring of $Ca^{2+}$ levels, a potentiometric sensor was made via depositing ZnO nanorods on Ag coated borosilicate-glass capillaries using a solution-based technique and then functionating with PVC membrane containing DB18C6 [83, 155]. The ZnO-modified electrode exhibited electrochemical potential changes of $Ca^{2+}$ concentration to an Ag/AgCl reference microelectrode. Initially, a buffer solution of $CaCl_2$ (pH ~ 7) was utilized for sensor calibration, and the linear potential difference through a broad concentration scale of 100 nM to 10 mM was obtained. The intracellular $Ca^{2+}$ concentrations estimations were performed in human fat cells and frog egg cells and identified to be 123 ± 23 nM and 250 ± 50 nM, respectively, which are in reasonable agreement with reported data [156, 157]. Based on SEM photographs of the functionalized electrode

after intracellular analysis, no trace of degradation of the ZnO nanorods was shown, which could associate with the impact of the polymeric membrane in protecting the ZnO surface [83]. Intracellular measurement of $K^+$ [83, 158] $Na^+$ [83, 159] and $Mg^{2+}$ [83, 160] was conducted applying the same techniques and, the ion-selective biosensors displayed reasonable sensitivity, stability, and selectivity in the existence of intrusive ions. The sensors performance demonstrates in Table (5).

A selective $Zn^{2+}$ ion biosensor using ZnO nanorods was deposited on gold-coated glassy electrodes by a low-temperature hydrothermal growth approach [161]. The as-deposited ZnO nanorods functionalized with plastic membrane coatings containing a certain zinc membrane (12-crown-4) in combination with PVC onto the surface of sensor. The $Zn^{2+}$ ion sensor was tested in PBS (pH = 7.4) and an excellent sensitivity of 35 mV/decade, a speedy response time of less than 5 s, and a low slight response to interfering ions (e.g., $Ca^{2+}$, $Mg^{2+}$, $K^+$, $Fe^{3+}$, and $Cu^{2+}$) were reported. The pH impact on the electrochemical signal was investigated in a 5-mM $Zn(NO_3)_2$ solution in the pH scale of (4 - 10). At pH ~ 7.4, the signal hit its maximum, whilst it decreased at lower pH values as a consequence of the membrane degradation in an acidic base. At larger values of pH, the signal reduced because of the ZnO decomposition.

**Table 5. Various electrodes employed in the production of metal ion biosensors using ZnO nanostructures.**

| Ion | Electrode | Sensitivity | Linear range | Detection limit | Response time | Ref. |
|---|---|---|---|---|---|---|
| $Ca^{2+}$ | DB18C6/ZnO nanorods /Ag wire EGFET | 113.92 mV/decade | 1 μM–1 mM | | 20 s | 154 |
| $Ca^{2+}$ | DB18C6/ZnO nanorods /Ag-coated glass capillary | 29.67 mV/decade | 100nM–10 mM | | | 194 |
| $Ca^{2+}$ | DB18C6/ZnO nanorods/Ag wire | 26.55 mV/decade | 0.1 μM–0.1 M | | < 1 min | 155 |
| $K^+$ | valinomycin /ZnO nanowires/ Ag-coated glass capillary | 41.5 mV/decade | 25 μM –125 mM | 1 μM | < 30 s | 195 |
| $Na^+$ | ETH 227/ZnO nanorods/ Ag-coated glass capillary | 72 mV/decade | 0.5mM–100 mM | | | 159 |
| $Mg^{2+}$ | Bz2dmit/ZnO nanorods/ Ag-coated glass capillary | 26.1 mV/decade | 500nM–100 mM | | | 160 |
| $Zn^{2+}$ | 12-crown-4/ZnO nanorods/Au-coated glassy electrode | ~35 mV/decade | 1 μM –100 mM | | < 5 s | 161 |
| $Sr^{2+}$ | ST/ZnO nanorods/Au-coated glassy electrode | 28.65 mV/decade | $1\times10^{-6}$–$5\times10^{-2}$M | | 10 s | 196 |
| $Fe^{3+}$ | 18 crown 6/ZnO nanorods/Ag wire | 70.12 mV/decade | $10^{-6}$–$10^{-2}$ M | | | 197 |
| $Tl^{+1}$ | DBzDA18C6/ ZnO nanorods/ Au-coated glass substrate | 36.87 mV/decade | | | < 5 s | 198 |
| $Pb^{+2}$ | $Fe_2O_3$NPs/ZnONRs/ITO | 4.40 μA $\mu M^{-1}$ | 0.2 μM –1.2 μM | 0.01 μM | | 209 |
| | | | | | | |

### 4. 6. ZnO Nanostructures based pH biosensors

The pH amount is an indicator of acidity or alkalinity of the aqueous solution, and it can influence the nutrients availability, biological functions, microbial activity. Owing to the significance of pH, the monitoring and controlling of its value is quite fundamental in most industrial, medical, and environmental applications, particularly in the food and beverage production as well as cosmetic and pharmaceutical manufacturing. ZnO nanostructures have been intensively applied in brilliant pH sensing systems because of the large surface-to-volume area, nontoxicity, chemical and photochemical stability, electrochemical activity, biocompatibility, outstanding amphoteric characteristics (interacting with both acidic and basic mediums), high viscosity, and ease fabrication. The fabrication strategy of pH sensor based ZnO nanostructures depends on a difference in surface potential at the ZnO/liquid interface. The highly dense adsorption sites for $H^+$ and $OH^-$ ions on the ZnO surface might serve as proton donors or acceptors, resulting in an electrochemical potential response of ZnO nanostructures to changes in pH value.

The pH sensors using ZnO nanorods, [162, 163, 164, 165] nanotubes, [ 162] nanowalls,[166] nanowires,[167] and nanoflakes [167] have been produced. Quantitative measurements [162, 168] contingent on the site-binding model [169] of the detection findings of ZnO nanorod based pH sensor have expected the highest Nernstian sensitivity of 59.1 mV/pH at 25°C in the large pH region (1 -14). In another study, the pH monitoring based on an individual ZnO nanorod was reported [170]. It found that a variation in surface potential at the ZnO/solution interface was identified as a linear change in conductance of the individual nanorod in the pH scale (2 -12) of 8.5 nS/ pH with a resolution of ~0.1 pH. It reported that the pH sensing performance was significantly affected by the structural properties and surface morphology (i.e., surface site density) of ZnO nanostructures [165, 168]. Since the broader surface-to-volume ratio ZnO nanowires exhibited superlative sensitivity of 36.65 mV/pH compared to that of 34.74 mV/pH for the nanowires–nanoflakes hybrids [167]. Furthermore, because of the broader surface-to-volume area with the existence of surface and subsurface oxygen vacancies, ZnO nanotubes produce sensitivity (45.9 mV/pH) as high as twice that of ZnO nanorods (28.4 mV/pH) [162].

The electrochemical potentials of the nanotube- and nanorod-based electrodes demonstrated a linear dependency on the pH value in the scale of (4-12) as demonstrated in Figure 12. An adjustable pH sensor using ZnO nanowalls on an extended gate thin film transistor was synthesized [166]. It was reported that sensitivity was in the vicinity of the optimum Nernstian value of 59 mV/pH, which was associated to the large surface-to-volume area of the nanowalls and also their surface deformities that performing as binding sites for surface proton reactions. Apart from the topography structural features, chemical adjustment of ZnO nanostructures could improve the sensor stability and increase its pH monitoring range [163, 167]. It was noticed that etching bare ZnO nanorods in an acidic solution (pH = 4.3) resulting in preventing pH sensing [163]. To deal with a such difficulty, the nanorods were functionalized with 3-aminopropyltriethoxysilane (APTES), which inhibited the ZnO etching in both acid and basic mediums and boosted pH sensing. The device monitored pH in the scale of (4.3-9.2) with enhanced sensitivity of 50.1 mV/pH. The same approach was used for APTES-modified ZnO nanostructures to increase the sensitivity and obtain a pH signal at 2 [167], which was impossible for bare ZnO (see Table 6).

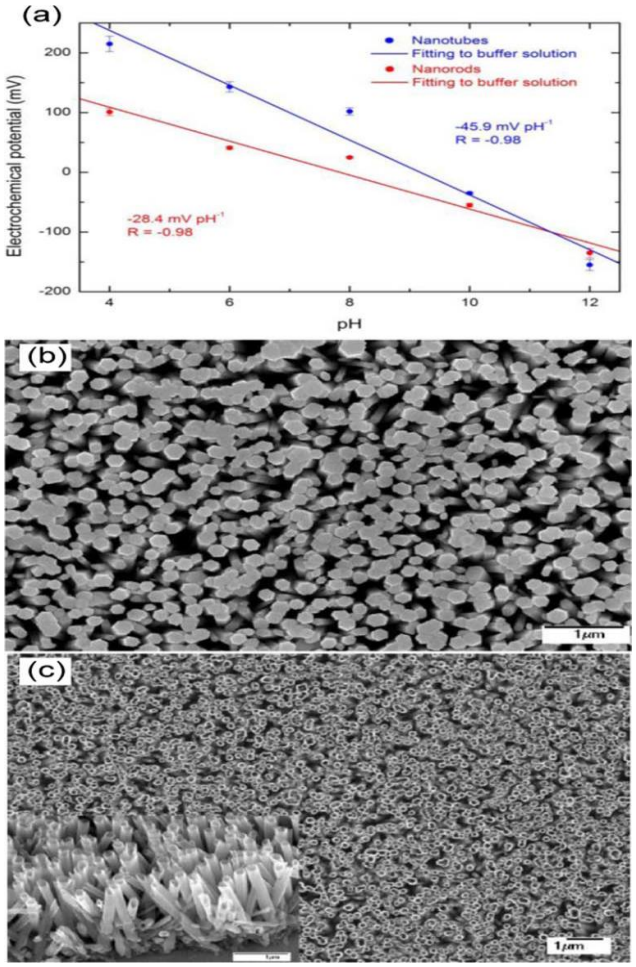


**Figure. 12:** (a) The analysis of electrochemical potential response vs pH for ZnO nanorods and nanotubes. SEM photographs of ZnO (b) nanorods and (c) nanotubes [162].

Moreover, it was reported that Al-doped ZnO nanostructures showed excellent pH sensitivity [171, 172]. The pH sensing performance depended on the Al concentration, as the device showed an excellent sensitivity of 57.95 mV/pH for Al-doped ZnO in contrast to 35 mV/pH for undoped ZnO in a broad scale of pH (1-13). An extremely sensitive pH sensor for testing in the vivo pH measurements in a human fat cell was developed [165]. An intracellular working electrode of ZnO nanorods with 80 nm diameter and 700 nm length exhibited an electrochemical potential variation against the Ag/AgCl intracellular reference microelectrode. The device exhibited an elevated sensitivity of 51.881 mV/pH at 22°C for a pH scale of (4–11). Moreover, the sensor was applied for pH intracellular analysis in a single human adipocyte or fat cell (Fig. 13) [165]. The working and reference electrodes were smoothly introduced through the cell membrane by hydraulic fine adjustments. Once the ZnO nanorods based electrode was included into the cell, the signal was recorded. The observed pH value of 6.81 was close to the intracellular pH values in rat brown adipocytes (6.95–7.57) [173] or at hepatocytes (6.85–7.05) [174] evaluated by applying indirect estimation of pH. It was observed that the cellular viability did not influence by the insertion of the electrodes into a single cell's cytoplasm for the pH intracellular measurements.

**Table 6. Various electrodes applied in the production of PH biosensors using ZnO nanostructures.**

| Electrode | Sensitivity mV/pH | Linear PH range | Response time | Ref. |
|---|---|---|---|---|
| ZnO nanowalls based EGTFT | ~59 | 1–9 | | 166 |
| APTES-modified ZnO nanorods/SiO2/Si substrates | 50.1 | 4.3–9.2 | | 163 |
| ZnO nanowires based EGFET | 36.65 | 4–9 | | 167 |
| ZnO nanowires-nanoflakes based EGFET | 34.74 | 4–9 | | 167 |
| APTES-modified ZnO nanowires-based EGFET | 43.22 | 2–9 | | 167 |
| APTES-modified ZnO nanowires-nanoflakes based EGFET | 41.58 | 2–9 | | 167 |
| AZO nanostructures based EGFET | 57.95 | 1–13 | | 172 |
| ZnO nanorods/borosilicate glass capillary | 51.881 | 4–11 | | 164 |
| ZnO nanorods /Au/Cr/glass | 28.4 | 4–12 | <100 s | 162 |
| ZnO nanotubes /Au/Cr/glass | 45.9 | 4–12 | <100 s | 162 |
| ZnO nanorods-based EGFET | 15.4 | 4–12 | | 199 |
| ZnO nanorods /Ag/glass | 44.56 | 4, 6, 7, 8, 10 | | 200 |
| ZnO film /Ag/glass | 34.82 | 4, 6, 7, 8, 10 | | 202 |
| ZnO/SiNW hybrid based EGFET | 66 | | | 201 |
| ZnO NRs based EG-FET | 24.67mV/pH$^{-1}$ | 0.98 – 0.99 | | 210 |
| Pt(NPs)/ ZnO NRs based EG-FET | 28.95mV pH$^{-1}$ | 0.99– 0.978 | | 211 |

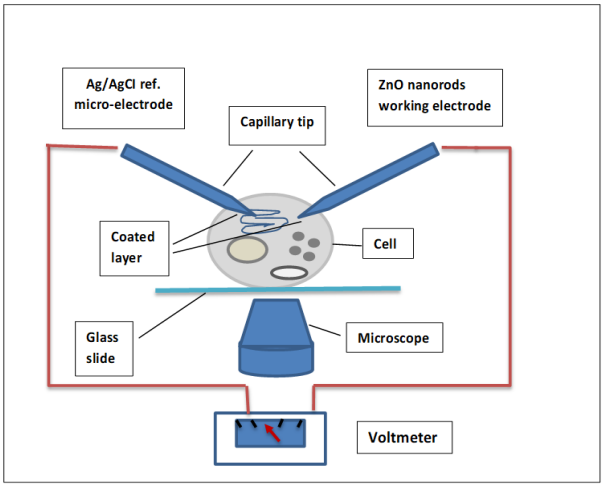


**Figure. 13:** Schematic illustration of intracellular pH measurements using ZnO nanorods as a working electrode with an Ag/AgCl reference microelectrode [165].

## 5. Conclusions

The rapid-growing development of biocompatible, biodegradable, and functionalized ZnO nanostructures allow those materials to be the building block for nanoplatforms or devices related to different promising and novel applications. Furthermore, the high electron transport rate and catalytic activity exhibited by ZnO nanostructures have expedited the fabrication of ZnO-based sensor devices toward their biomedical applications. Detection of many metal ions and critical physiological components, including glucose, cholesterol, L-lactate, uric acid, and others has been explained utilizing ZnO high-performance sensing platforms. Moreover, improving performance and efficiency, increasing sensitivity and selectivity, less response time, broad linear response ranges, reproducibility, and low detection limits to detect single biomolecules have been proven for several categories of analytes.

Even with recent progress, many obstacles still needed to be overcome, specifically in terms of bringing ZnO-based biosensors from the laboratory to be scaled up and implemented in a broad range of healthcare systems and disease diagnoses. One of the most challenges is the toxicological impact of ZnO nanostructures which is not fully understood and covered in the literature. Moreover, the capability to efficiently capture biorecognition signals and transform them into measurable and detectable signals is critical for the biosensor performance. A multidisciplinary approach should systematically integrate to address all fundamental difficulties and build low cost, miniaturized, commercially available, portable, intelligent ZnO nanostructures-based biosensors.

## Abbreviations and Acronyms

| | |
|---|---|
| point-of-care | POC |
| Field Effect Transistor | FET |
| Magnetic Resonance Imaging | MRI |
| Ribonucleic Acid | RNA |
| Deoxyribonucleic Acid | DNA |
| Circulating Tumour Cells | CTCs |
| Isoelectric Point | IEP |
| Glucose Oxidase | GOx |
| Phosphate Buffered Saline | PBS |
| Indium Tin Oxide | ITO |
| Carbon Nanotubes | CNTs |
| Cholesterol Oxidase | ChOx |
| Cholesterol Esterase | ChEt |
| Lactate Dehydrogenase | LDH |
| Lactate Oxidase | LOD |
| Polydiallyldimethyl Ammonium | PDDA |
| Multi Walled Carbon Nanotubes | MWCNTs |
| Bovine Serum Albumin | BSA |
| Pyrolytic Graphite | PG |
| Differential Pulse Voltammetry | DPV |
| Graphene Foam | GF |
| Polypyrrole | PPy |
| Polyaniline | PANI |
| Polyvinyl Chloride | PVC |
| Metal Oxide Semiconductor Field Effect Transistor | MOSFET |
| Aminopropyltriethoxysilane | APTES |

## References

[1]- Zhao, Z., Lei, W., Zhang, X., Wang, B. and Jiang, H., 2010. ZnO-based amperometric enzyme biosensors. *Sensors*, *10*(2), pp.1216-1231.

[2]- Grieshaber, D., MacKenzie, R., Vörös, J. and Reimhult, E., 2008. Electrochemical biosensors-sensor principles and architectures. *Sensors*, *8*(3), pp.1400-1458.

[3]- Wilson, M.S., 2005. Electrochemical immunosensors for the simultaneous detection of two tumor markers. *Analytical chemistry*, *77*(5), pp.1496-1502.

[4]- D'Orazio, P., 2003. Biosensors in clinical chemistry. *Clinica chimica acta*, *334*(1-2), pp.41-69.

[5]- Neumann, S., 2015. *Biomarkers–past and future* (pp. 1-22). Wiley

[6]- Turner, A.P., 2013. Biosensors: sense and sensibility. *Chemical Society Reviews*, *42*(8), pp.3184-3196.

[7]- Vadgama, P. and Crump, P.W., 1992. Biosensors: recent trends. A review. *Analyst*, *117*(11), pp.1657-1670.
[8]- Pai, N.P., Vadnais, C., Denkinger, C., Engel, N. and Pai, M., 2012. Point-of-care testing for infectious diseases: diversity, complexity, and barriers in low-and middle-income countries.
[9]- Lee, T.M.H., 2008. Over-the-counter biosensors: Past, present, and future. *Sensors*, *8*(9), pp.5535-5559.
[10]- Chin, C.D., Chin, S.Y., Laksanasopin, T. and Sia, S.K., 2013. Low-cost microdevices for point-of-care testing. In *Point-of-care diagnostics on a chip* (pp. 3-21). Springer, Berlin, Heidelberg.
[11]- Mehrotra, P., 2016. Biosensors and their applications–A review. *Journal of oral biology and craniofacial research*, *6*(2), pp.153-159.
[12]- Xu, M., Li, J., Iwai, H., Mei, Q., Fujita, D., Su, H., Chen, H. and Hanagata, N., 2012. Formation of nano-bio-complex as nanomaterials dispersed in a biological solution for understanding nanobiological interactions. *Scientific reports*, *2*(1), pp.1-6
[13]- Diamanti, S., Arifuzzaman, S., Elsen, A., Genzer, J. and Vaia, R.A., 2008. Reactive patterning via post-functionalization of polymer brushes utilizing disuccinimidyl carbonate activation to couple primary amines. *Polymer*, *49*(17), pp.3770-3779..
[14]- Balzani, V., 2005. Nanoscience and nanotechnology: a personal view of a chemist. *small*, *1*(3), pp.278-283.
[15]- Service, R.F., 2003. Nanodevices Make Fresh Strides Toward Reality.
[16]- Patolsky, F., Zheng, G. and Lieber, C.M., 2006. Nanowire sensors for medicine and the life sciences.
[17]- Carrara, S., Ghoreishizadeh, S., Olivo, J., Taurino, I., Baj-Rossi, C., Cavallini, A., Op de Beeck, M., Dehollain, C., Burleson, W., Moussy, F.G. and Guiseppi-Elie, A., 2012. Fully integrated biochip platforms for advanced healthcare. *Sensors*, *12*(8), pp.11013-11060.
[18]- Gooding, J.J., Lai, L.M. and Goon, I.Y., 2009. Nanostructured electrodes with unique properties for biological and other applications. *Advances in electrochemical science and engineering*, *11*.
[19]- Liu, X., Lin, P., Yan, X., Kang, Z., Zhao, Y., Lei, Y., Li, C., Du, H. and Zhang, Y., 2013. Enzyme-coated single ZnO nanowire FET biosensor for detection of uric acid. *Sensors and Actuators B: Chemical*, *176*, pp.22-27.
[20]- Naresh, V. and Lee, N., 2021. A review on biosensors and recent development of nanostructured materials-enabled biosensors. *Sensors*, *21*(4), p.1109.
[21]- Chaubey, A. and Malhotra, B., 2002. Mediated biosensors. *Biosensors and bioelectronics*, *17*(6-7), pp.441-456.
[22]- Eggins, B.R., 2008. Chemical sensors and biosensors. John Wiley & Sons.
[23]- Luppa, P.B., Sokoll, L.J. and Chan, D.W., 2001. Immunosensors—principles and applications to clinical chemistry. *Clinica chimica acta*, *314*(1-2), pp.1-26.
[24]- Wang, J., 2006. Electrochemical biosensors: towards point-of-care cancer diagnostics. *Biosensors and Bioelectronics*, *21*(10), pp.1887-1892.
[25]- Langer, R., 1998. Drug delivery and targeting. *Nature*, *392*(6679 Suppl), pp.5-10.
[26]- Caras, S. and Janata, J., 1980. Field effect transistor sensitive to penicillin. *Analytical chemistry*, *52*(12), pp.1935-1937.
[27]- Jaffrezic-Renault, N. and Dzyadevych, S.V., 2008. Conductometric microbiosensors for environmental monitoring. *Sensors*, *8*(4), pp.2569-2588.
[28]- Patolsky, F., Zheng, G. and Lieber, C.M., 2006. Nanowire-based biosensors.
[29]- Städler, B., Solak, H.H., Frerker, S., Bonroy, K., Frederix, F., Vörös, J. and Grandin, H.M., 2007. Nanopatterning of gold colloids for label-free biosensing. *Nanotechnology*, *18*(15), p.155306.
[30]- Yagiuda, K., Hemmi, A., Ito, S., Asano, Y., Fushinuki, Y., Chen, C.Y. and Karube, I., 1996. Development of a conductivity-based immunosensor for sensitive detection of methamphetamine (stimulant drug) in human urine. *Biosensors and Bioelectronics*, *11*(8), pp.703-707.
[31]- Morkoc, H. and Ozgur, U., 2009. General properties of ZnO, zinc oxide: fundamentals. *Materials and Device Technology*, pp.1-2.
[32]- Coleman, V.A. and Jagadish, C., 2006. Basic properties and applications of ZnO. In *Zinc oxide bulk, thin films and nanostructures* (pp. 1-20). Elsevier Science Ltd.
[33]- Rekha, K., Nirmala, M., Nair, M.G. and Anukaliani, A., 2010. Structural, optical, photocatalytic and antibacterial activity of zinc oxide and manganese doped zinc oxide nanoparticles. *Physica B: Condensed Matter*, *405*(15), pp.3180-3185.
[34]- Jeong, W.J., Kim, S.K. and Park, G.C., 2006. Preparation and characteristic of ZnO thin film with high and low resistivity for an application of solar cell. *Thin Solid Films*, *506*, pp.180-183.
[35]- Vanmaekelbergh, D. and Van Vugt, L.K., 2011. ZnO nanowire lasers. *Nanoscale*, *3*(7), pp.2783-2800.
[36]- Nair, S., Sasidharan, A., Rani, V.D., Menon, D., Nair, S., Manzoor, K. and Raina, S., 2009. Role of size scale of ZnO nanoparticles and microparticles on toxicity toward bacteria and osteoblast cancer cells. *Journal of Materials Science: Materials in Medicine*, *20*(1), p.235.
[37]- Reinert, A.A., Payne, C., Wang, L., Ciston, J., Zhu, Y. and Khalifah, P.G., 2013. Synthesis and characterization of visible light absorbing (GaN) 1–x (ZnO) x semiconductor nanorods. *Inorganic chemistry*, *52*(15), pp.8389-8398.
[38]- Zhang, Y., R Nayak, T., Hong, H. and Cai, W., 2013. Biomedical applications of zinc oxide nanomaterials. *Current molecular medicine*, *13*(10), pp.1633-1645.
[39]- Taratula, O., Galoppini, E., Wang, D., Chu, D., Zhang, Z., Chen, H., Saraf, G. and Lu, Y., 2006. Binding studies of molecular linkers to ZnO and MgZnO nanotip films. *The Journal of Physical Chemistry B*, *110*(13), pp.6506-6515.
[40]- Liu, D., Wu, W., Qiu, Y., Yang, S., Xiao, S., Wang, Q.Q., Ding, L. and Wang, J., 2008. Surface functionalization of ZnO nanotetrapods with photoactive and electroactive organic monolayers. *Langmuir*, *24*(9), pp.5052-5059.
[41]- Zhou, J., Xu, N.S. and Wang, Z.L., 2006. Dissolving behavior and stability of ZnO wires in biofluids: a study on biodegradability and biocompatibility of ZnO nanostructures. *Advanced Materials*, *18*(18), pp.2432-2435.
[42]- Bisht, G. and Rayamajhi, S., 2016. ZnO nanoparticles: a promising anticancer agent. *Nanobiomedicine*, *3*(Godište 2016), pp.3-9.
[43]- Smalley, K.S. and Herlyn, M., 2006. Towards the targeted therapy of melanoma. *Mini reviews in medicinal chemistry*, *6*(4), pp.387-393.
[44]- Gowda, R., Jones, N.R., Banerjee, S. and Robertson, G.P., 2013. Use of nanotechnology to develop multi-drug inhibitors for cancer therapy. *Journal of nanomedicine & nanotechnology*, *4*(6).
[45]- McNeil, S.E., 2009. Nanoparticle therapeutics: a personal perspective. *Wiley Interdisciplinary Reviews: Nanomedicine and Nanobiotechnology*, *1*(3), pp.264-271.
[46]- Kim, W., Ng, J.K., Kunitake, M.E., Conklin, B.R. and Yang, P., 2007. Interfacing silicon nanowires with mammalian cells. *Journal of the American Chemical Society*, *129*(23), pp.7228-7229.
[47]- Rahong, S., Yasui, T., Kaji, N. and Baba, Y., 2016. Recent developments in nanowires for bio-applications from molecular to cellular levels. *Lab on a Chip*, *16*(7), pp.1126-1138.
[48]- Hanley, C., Layne, J., Punnoose, A., Reddy, K., Coombs, I., Coombs, A., Feris, K. and Wingett, D., 2008. Preferential killing of cancer cells and activated human T cells using ZnO nanoparticles. *Nanotechnology*, *19*(29), p.295103.
[49]- Shen, C., James, S.A., de Jonge, M.D., Turney, T.W., Wright, P.F. and Feltis, B.N., 2013. Relating cytotoxicity, zinc ions, and reactive oxygen in ZnO nanoparticle–exposed human immune cells. *Toxicological Sciences*, *136*(1), pp.120-130.
[50]- Rasmussen, J.W., Martinez, E., Louka, P. and Wingett, D.G., 2010. Zinc oxide nanoparticles for selective destruction of tumor cells and potential for drug delivery applications. *Expert opinion on drug delivery*, *7*(9), pp.1063-1077.

[51]- Wang, H., Wingett, D., Engelhard, M.H., Feris, K., Reddy, K.M., Turner, P., Layne, J., Hanley, C., Bell, J., Tenne, D. and Wang, C., 2009. Fluorescent dye encapsulated ZnO particles with cell-specific toxicity for potential use in biomedical applications. *Journal of Materials Science: Materials in Medicine*, *20*(1), pp.11-22.

[52]- H. Müller, K., Kulkarni, J., Motskin, M., Goode, A., Winship, P., Skepper, J.N., Ryan, M.P. and Porter, A.E., 2010. pH-dependent toxicity of high aspect ratio ZnO nanowires in macrophages due to intracellular dissolution. *ACS nano*, *4*(11), pp.6767-6779.

[53]- Tilke, A.T., Simmel, F.C., Lorenz, H., Blick, R.H. and Kotthaus, J.P., 2003. Quantum interference in a one-dimensional silicon nanowire. *Physical Review B*, *68*(7), p.075311.

[54]- Khanal, D.R., Yim, J.W., Walukiewicz, W. and Wu, J., 2007. Effects of quantum confinement on the doping limit of semiconductor nanowires. *Nano letters*, *7*(5), pp.1186-1190.

[55]- Wang, J.X., Sun, X.W., Wei, A., Lei, Y., Cai, X.P., Li, C.M. and Dong, Z.L., 2006. Zinc oxide nanocomb biosensor for glucose detection. *Applied physics letters*, *88*(23), p.233106.

[56]- Yakimova, R., Selegård, L., Khranovskyy, V., Pearce, R., Lloyd Spetz, A. and Uvdal, K., 2012. ZnO materials and surface tailoring for biosensing. *Frontiers in bioscience (Elite edition)*, *4*(1), pp.254-278.

[57]- Alberts, B., 2017. Molecular Biology of the Cell (MBoC). *Garland Science*.

[58]- Asif, M.H., Ali, S.M.U., Nur, O., Willander, M., Brännmark, C., Strålfors, P., Englund, U.H., Elinder, F. and Danielsson, B., 2010. Functionalised ZnO-nanorod-based selective electrochemical sensor for intracellular glucose. *Biosensors and Bioelectronics*, *25*(10), pp.2205-2211.

[59]- Chaniotakis, N.A., 2004. Enzyme stabilization strategies based on electrolytes and polyelectrolytes for biosensor applications. *Analytical and Bioanalytical Chemistry*, *378*(1), pp.89-95.

[60]- Yang, Z., Ye, Z., Zhao, B., Zong, X. and Wang, P., 2010. Synthesis of ZnO nanobundles via Sol–Gel route and application to glucose biosensor. *Journal of sol-gel science and technology*, *54*(3), pp.282-285.

[61]- Feng, X., Liu, Y., Kong, Q., Ye, J., Chen, X., Hu, J. and Chen, Z., 2010. Direct electrochemistry of myoglobin immobilized on chitosan-wrapped rod-constructed ZnO microspheres and its application to hydrogen peroxide biosensing. *Journal of Solid State Electrochemistry*, *14*(6), pp.923-930.

[62]- Kuznetsov, B.A., Shumakovich, G.P., Koroleva, O.V. and Yaropolov, A.I., 2001. On applicability of laccase as label in the mediated and mediatorless electroimmunoassay: effect of distance on the direct electron transfer between laccase and electrode. *Biosensors and Bioelectronics*, *16*(1-2), pp.73-84

[63]- Fang, A., Ng, H.T. and Li, S.F.Y., 2003. A high-performance glucose biosensor based on monomolecular layer of glucose oxidase covalently immobilised on indium–tin oxide surface. *Biosensors and bioelectronics*, *19*(1), pp.43-49..

[64]- Nel, A.E., Mädler, L., Velegol, D., Xia, T., Hoek, E.M., Somasundaran, P., Klaessig, F., Castranova, V. and Thompson, M., 2009. Understanding biophysicochemical interactions at the nano–bio interface. *Nature materials*, *8*(7), pp.543-557.

[65]- Min, Y., Akbulut, M., Kristiansen, K., Golan, Y. and Israelachvili, J., 2010. The role of interparticle and external forces in nanoparticle assembly. *Nanoscience And Technology: A collection of reviews from Nature journals*, pp.38-49.

[66]- Geiser, M., Rothen-Rutishauser, B., Kapp, N., Schürch, S., Kreyling, W., Schulz, H., Semmler, M., Hof, V.I., Heyder, J. and Gehr, P., 2005. Ultrafine particles cross cellular membranes by nonphagocytic mechanisms in lungs and in cultured cells. *Environmental health perspectives*, *113*(11), pp.1555-1560.

[67]- Rimai, D.S., Quesnel, D.J. and Busnaina, A.A., 2000. The adhesion of dry particles in the nanometer to micrometer-size range. *Colloids and surfaces A: Physicochemical and engineering aspects*, *165*(1-3), pp.3-10.

[68]- Clark Jr, L.C. and Lyons, C., 1962. Electrode systems for continuous monitoring in cardiovascular surgery. *Annals of the New York Academy of sciences*, *102*(1), pp.29-45.

[69]- Wei, A., Sun, X.W., Wang, J.X., Lei, Y., Cai, X.P., Li, C.M., Dong, Z.L. and Huang, W., 2006. Enzymatic glucose biosensor based on ZnO nanorod array grown by hydrothermal decomposition. *Applied Physics Letters*, *89*(12), p.123902.

[70]- Umar, A., Rahman, M.M., Kim, S.H. and Hahn, Y.B., 2008. ZnO nanonails: synthesis and their application as glucose biosensor. *Journal of Nanoscience and Nanotechnology*, *8*(6), pp.3216-3221.

[71]- Ali, S.M.U., Nur, O., Willander, M. and Danielsson, B., 2010. A fast and sensitive potentiometric glucose microsensor based on glucose oxidase coated ZnO nanowires grown on a thin silver wire. *Sensors and Actuators B: Chemical*, *145*(2), pp.869-874.

[72]- Fulati, A., Ali, S.M.U., Asif, M.H., Willander, M., Brännmark, C., Strålfors, P., Börjesson, S.I., Elinder, F. and Danielsson, B., 2010. An intracellular glucose biosensor based on nanoflake ZnO. *Sensors and Actuators B: Chemical*, *150*(2), pp.673-680.

[73]- Zhou, F., Jing, W., Wu, Q., Gao, W., Jiang, Z., Shi, J. and Cui, Q., 2016. Effects of the surface morphologies of ZnO nanotube arrays on the performance of amperometric glucose sensors. *Materials Science in Semiconductor Processing*, *56*, pp.137-144.

[74]- Ahmad, M., Pan, C., Luo, Z. and Zhu, J., 2010. A single ZnO nanofiber-based highly sensitive amperometric glucose biosensor. *The Journal of Physical Chemistry C*, *114*(20), pp.9308-9313.

[75]- Liu, X., Hu, Q., Wu, Q., Zhang, W., Fang, Z. and Xie, Q., 2009. Aligned ZnO nanorods: a useful film to fabricate amperometric glucose biosensor. *Colloids and Surfaces B: Biointerfaces*, *74*(1), pp.154-158.

[76]- Liu, J., Guo, C., Li, C.M., Li, Y., Chi, Q., Huang, X., Liao, L. and Yu, T., 2009. Carbon-decorated ZnO nanowire array: A novel platform for direct electrochemistry of enzymes and biosensing applications. *Electrochemistry Communications*, *11*(1), pp.202-205.

[77]- Pollock, A.S., 1984. Intracellular pH of hepatocytes in primary monolayer culture. *American Journal of Physiology-Renal Physiology*, *246*(5), pp.F738-F744.

[78]- Ren, X., Chen, D., Meng, X., Tang, F., Hou, X., Han, D. and Zhang, L., 2009. Zinc oxide nanoparticles/glucose oxidase photoelectrochemical system for the fabrication of biosensor. *Journal of colloid and interface science*, *334*(2), pp.183-187.

[79]- Hwa, K.Y. and Subramani, B., 2014. Synthesis of zinc oxide nanoparticles on graphene–carbon nanotube hybrid for glucose biosensor applications. *Biosensors and Bioelectronics*, *62*, pp.127-133.

[80]- Karuppiah, C., Palanisamy, S., Chen, S.M., Veeramani, V. and Periakaruppan, P., 2014. Direct electrochemistry of glucose oxidase and sensing glucose using a screen-printed carbon electrode modified with graphite nanosheets and zinc oxide nanoparticles. *Microchimica Acta*, *181*(15-16), pp.1843-1850.

[81]- Ahmad, R., Tripathy, N., Kim, J.H. and Hahn, Y.B., 2012. Highly selective wide linear-range detecting glucose biosensors based on aspect-ratio controlled ZnO nanorods directly grown on electrodes. *Sensors and Actuators B: Chemical*, *174*, pp.195-201.

[82]- Aini, B.N., Siddiquee, S., Ampon, K., Rodrigues, K.F. and Suryani, S., 2015. Development of glucose biosensor based on ZnO nanoparticles film and glucose oxidase-immobilized eggshell membrane. *Sensing and Bio-Sensing Research*, *4*, pp.46-56.

[83]- Asif, M.H., Danielsson, B. and Willander, M., 2015. ZnO nanostructure-based intracellular sensor. *Sensors*, *15*(5), pp.11787-11804.

[84]- Kong, T., Chen, Y., Ye, Y., Zhang, K., Wang, Z. and Wang, X., 2009. An amperometric glucose biosensor based on the immobilization of glucose oxidase on the ZnO nanotubes. *Sensors and Actuators B: Chemical*, *138*(1), pp.344-350.

[85]- Jing, W.X., Zhou, F., Gao, W.Z., Jiang, Z.D., Ren, W., Shi, J.F., Cheng, Y.Y. and Gao, K., 2015. Regulating the hydrothermal synthesis of ZnO nanorods to optimize the performance of

spirally hierarchical structure-based glucose sensors. *RSC advances*, *5*(105), pp.85988-85995.

[86]- Miao, F., Lu, X., Tao, B., Li, R. and Chu, P.K., 2016. Glucose oxidase immobilization platform based on ZnO nanowires supported by silicon nanowires for glucose biosensing. *Microelectronic Engineering*, *149*, pp.153-158.

[87]- Zhang, Y., Xu, J., Xiang, Q., Li, H., Pan, Q. and Xu, P., 2009. Brush-like hierarchical ZnO nanostructures: synthesis, photoluminescence and gas sensor properties. *The Journal of Physical Chemistry C*, *113*(9), pp.3430-3435.

[88]- Fan, S., Zhao, M., Ding, L., Ma, Y., Liang, J., Wang, X., Song, Y. and Chen, S., 2016. Introducing pn junction interface into enzyme loading matrix for enhanced glucose biosensing performance. *Sensors and Actuators B: Chemical*, *237*, pp.373-379.

[89]- Izyumskaya, N., Tahira, A., Ibupoto, Z.H., Lewinski, N., Avrutin, V., Özgür, Ü., Topsakal, E., Willander, M. and Morkoç, H., 2017. Electrochemical biosensors based on ZnO nanostructures. *ECS Journal of Solid State Science and Technology*, *6*(8), p.Q84.

[90]- Fang, L., Liu, B., Liu, L., Li, Y., Huang, K. and Zhang, Q., 2016. Direct electrochemistry of glucose oxidase immobilized on Au nanoparticles-functionalized 3D hierarchically ZnO nanostructures and its application to bioelectrochemical glucose sensor. *Sensors and Actuators B: Chemical*, *222*, pp.1096-1102.

[91]- Tian, K., Alex, S., Siegel, G. and Tiwari, A., 2015. Enzymatic glucose sensor based on Au nanoparticle and plant-like ZnO film modified electrode. *Materials Science and Engineering: C*, *46*, pp.548-552.

[92]- Wei, Y., Li, Y., Liu, X., Xian, Y., Shi, G. and Jin, L., 2010. ZnO nanorods/Au hybrid nanocomposites for glucose biosensor. *Biosensors and Bioelectronics*, *26*(1), pp.275-278.

[93]- Mazeiko, V., Kausaite-Minkstimiene, A., Ramanaviciene, A., Balevicius, Z. and Ramanavicius, A., 2013. Gold nanoparticle and conducting polymer-polyaniline-based nanocomposites for glucose biosensor design. *Sensors and Actuators B: Chemical*, *189*, pp.187-193.

[94]- Kim, J.Y., Jo, S.Y., Sun, G.J., Katoch, A., Choi, S.W. and Kim, S.S., 2014. Tailoring the surface area of ZnO nanorods for improved performance in glucose sensors. *Sensors and Actuators B: Chemical*, *192*, pp.216-220.

[95]- Toghill, K.E. and Compton, R.G., 2010. Electrochemical non-enzymatic glucose sensors: a perspective and an evaluation. *Int. J. Electrochem. Sci*, *5*(9), pp.1246-1301.

[96]- Zeng, S., Yong, K.T., Roy, I., Dinh, X.Q., Yu, X. and Luan, F., 2011. A review on functionalized gold nanoparticles for biosensing applications. *Plasmonics*, *6*(3), pp.491-506.

[97]- Lin, S.Y., Chang, S.J. and Hsueh, T.J., 2014. ZnO nanowires modified with Au nanoparticles for nonenzymatic amperometric sensing of glucose. *Applied Physics Letters*, *104*(19), p.193704.

[98]- Hsu, C.L., Lin, J.H., Hsu, D.X., Wang, S.H., Lin, S.Y. and Hsueh, T.J., 2017. Enhanced non-enzymatic glucose biosensor of ZnO nanowires via decorated Pt nanoparticles and illuminated with UV/green light emitting diodes. *Sensors and Actuators B: Chemical*, *238*, pp.150-159.

[99]- Vijayaprasath, G., Murugan, R., Narayanan, J.S., Dharuman, V., Ravi, G. and Hayakawa, Y., 2015. Glucose sensing behavior of cobalt doped ZnO nanoparticles synthesized by co-precipitation method. *Journal of Materials Science: Materials in Electronics*, *26*(7), pp.4988-4996.

[100]- Park, S., Cho, K. and Kim, S., 2011. Enzyme-free glucose sensors with channels composed of necked ZnO nanoparticles on plastic. *Microelectronic engineering*, *88*(8), pp.2611-2613.

[101]- Zhou, F., Jing, W., Liu, P., Han, D., Jiang, Z. and Wei, Z., 2017. Doping Ag in ZnO nanorods to improve the performance of related enzymatic glucose sensors. *Sensors*, *17*(10), p.2214.

[102]- Tian, K., Prestgard, M. and Tiwari, A., 2014. A review of recent advances in nonenzymatic glucose sensors. *Materials Science and Engineering: C*, *41*, pp.100-118.

[103]- Yang, J., Cho, M. and Lee, Y., 2016. Synthesis of hierarchical Ni (OH) 2 hollow nanorod via chemical bath deposition and its glucose sensing performance. *Sensors and Actuators B: Chemical*, *222*, pp.674-681.

[104]- Strano, V. and Mirabella, S., 2016. Hierarchical ZnO nanorods/Ni (OH) 2 nanoflakes for room-temperature, cheap fabrication of non-enzymatic glucose sensors. *RSC advances*, *6*(112), pp.111374-111379.

[105]- Zhou, C., Xu, L., Song, J., Xing, R., Xu, S., Liu, D. and Song, H., 2014. Ultrasensitive non-enzymatic glucose sensor based on three-dimensional network of ZnO-CuO hierarchical nanocomposites by electrospinning. *Scientific reports*, *4*(1), pp.1-9.

[106]- Ding, Y., Wang, Y., Su, L., Zhang, H. and Lei, Y., 2010. Preparation and characterization of NiO–Ag nanofibers, NiO nanofibers, and porous Ag: towards the development of a highly sensitive and selective non-enzymatic glucose sensor. *Journal of Materials Chemistry*, *20*(44), pp.9918-9926.

[107]- SoYoon, S., Ramadoss, A., Saravanakumar, B. and Kim, S.J., 2014. Novel Cu/CuO/ZnO hybrid hierarchical nanostructures for non-enzymatic glucose sensor application. *Journal of Electroanalytical Chemistry*, *717*, pp.90-95.

[108]- Wu, J. and Yin, F., 2013. Easy fabrication of a sensitive non-enzymatic glucose sensor based on electrospinning CuO-ZnO nanocomposites. *Integrated Ferroelectrics*, *147*(1), pp.47-58.

[109]- Niu, X., Li, X., Pan, J., He, Y., Qiu, F. and Yan, Y., 2016. Recent advances in non-enzymatic electrochemical glucose sensors based on non-precious transition metal materials: opportunities and challenges. *RSC advances*, *6*(88), pp.84893-84905.

[110]- Motonaka, J. and Faulkner, L.R., 1993. Determination of cholesterol and cholesterol ester with novel enzyme microsensors. *Analytical chemistry*, *65*(22), pp.3258-3261.

[111]- Umar, A., Rahman, M.M., Vaseem, M. and Hahn, Y.B., 2009. Ultra-sensitive cholesterol biosensor based on low-temperature grown ZnO nanoparticles. *Electrochemistry Communications*, *11*(1), pp.118-121.

[112]- Ahmad, M., Pan, C., Gan, L., Nawaz, Z. and Zhu, J., 2010. Highly sensitive amperometric cholesterol biosensor based on Pt-incorporated fullerene-like ZnO nanospheres. *The Journal of Physical Chemistry C*, *114*(1), pp.243-250.

[113]- Psychoyios, V.N., Nikoleli, G.P., Tzamtzis, N., Nikolelis, D.P., Psaroudakis, N., Danielsson, B., Israr, M.Q. and Willander, M., 2013. Potentiometric cholesterol biosensor based on ZnO nanowalls and stabilized polymerized lipid film. *Electroanalysis*, *25*(2), pp.367-372.

[114]- Ahmad, R., Tripathy, N., Kim, S.H., Umar, A., Al-Hajry, A. and Hahn, Y.B., 2014. High performance cholesterol sensor based on ZnO nanotubes grown on Si/Ag electrodes. *Electrochemistry communications*, *38*, pp.4-7.

[115]- Wang, C., Tan, X., Chen, S., Yuan, R., Hu, F., Yuan, D. and Xiang, Y., 2012. Highly-sensitive cholesterol biosensor based on platinum–gold hybrid functionalized ZnO nanorods. *Talanta*, *94*, pp.263-270.

[116]- Mahmoud, A., Echabaane, M., Omri, K., El Mir, L. and Chaabane, R.B., 2019. Development of an impedimetric non enzymatic sensor based on ZnO and Cu doped ZnO nanoparticles for the detection of glucose. *Journal of Alloys and Compounds*, *786*, pp.960-968.

[117]- Hayat, A., Haider, W., Raza, Y. and Marty, J.L., 2015. Colorimetric cholesterol sensor based on peroxidase like activity of zinc oxide nanoparticles incorporated carbon nanotubes. *Talanta*, *143*, pp.157-161.

[118]- Umar, A., Rahman, M.M., Al-Hajry, A. and Hahn, Y.B., 2009. Highly-sensitive cholesterol biosensor based on well-crystallized flower-shaped ZnO nanostructures. *Talanta*, *78*(1), pp.284-289.

[119]- Ahmad, R., Tripathy, N. and Hahn, Y.B., 2012. Wide linear-range detecting high sensitivity cholesterol biosensors based on aspect-ratio controlled ZnO nanorods grown on silver electrodes. *Sensors and Actuators B: Chemical*, *169*, pp.382-386.

[120]- Batra, N., Tomar, M. and Gupta, V., 2012. Realization of an efficient cholesterol biosensor using ZnO nanostructured thin film. *Analyst*, *137*(24), pp.5854-5859.

[121]- Batra, N., Tomar, M. and Gupta, V., 2014. ZnO Nanostructured Thin Film as an Efficient Matrix for Total Cholesterol Detection. *Advanced Science Letters*, *20*(5-6), pp.1044-1049.

[122]- Solanki, P.R., Kaushik, A., Ansari, A.A. and Malhotra, B.D., 2009. Nanostructured zinc oxide platform for cholesterol sensor. *Applied Physics Letters*, *94*(14), p.143901.

[123]- Wu, Q., Hou, Y., Zhang, M., Hou, X., Xu, L., Wang, N., Wang, J. and Huang, W., 2016. Amperometric cholesterol biosensor based on zinc oxide films on a silver nanowire–graphene oxide modified electrode. *Analytical Methods*, *8*(8), pp.1806-1812.

[124]- Giri, A.K., Charan, C., Ghosh, S.C., Shahi, V.K. and Panda, A.B., 2016. Phase and composition selective superior cholesterol sensing performance of ZnO@ ZnS nano-heterostructure and ZnS nanotubes. *Sensors and Actuators B: Chemical*, *229*, pp.14-24.

[125]- Giri, A.K., Charan, C., Saha, A., Shahi, V.K. and Panda, A.B., 2014. An amperometric cholesterol biosensor with excellent sensitivity and limit of detection based on an enzyme-immobilized microtubular ZnO@ ZnS heterostructure. *Journal of Materials Chemistry A*, *2*(40), pp.16997-17004.

[126]- Vilian, A.E., Chen, S.M., Kwak, C.H., Hwang, S.K., Huh, Y.S. and Han, Y.K., 2016. Immobilization of hemoglobin on functionalized multi-walled carbon nanotubes-poly-l-histidine-zinc oxide nanocomposites toward the detection of bromate and H2O2. *Sensors and Actuators B: Chemical*, *224*, pp.607-617.

[127]- Kreisberg, R.A., 1984. Pathogenesis and management of lactic acidosis. *Annual review of medicine*, *35*(1), pp.181-193.

[128]- Phypers, B. and Pierce, J.T., 2006. Lactate physiology in health and disease. *Continuing education in Anaesthesia, critical care & pain*, *6*(3), pp.128-132.

[129]- Ibupoto, Z.H., Shah, S.M.U.A., Khun, K. and Willander, M., 2012. Electrochemical L-lactic acid sensor based on immobilized ZnO nanorods with lactate oxidase. *Sensors*, *12*(3), pp.2456-2466.

[130]- Lei, Y., Luo, N., Yan, X., Zhao, Y., Zhang, G. and Zhang, Y., 2012. A highly sensitive electrochemical biosensor based on zinc oxide nanotetrapods for L-lactic acid detection. *Nanoscale*, *4*(11), pp.3438-3443.

[131]- Kobayashi, K.U.M.P.E.I. and Neely, J.R., 1979. Control of maximum rates of glycolysis in rat cardiac muscle. *Circulation Research*, *44*(2), pp.166-175.

[132]- Shapiro, F. and Silanikove, N., 2010. Rapid and accurate determination of D-and L-lactate, lactose and galactose by enzymatic reactions coupled to formation of a fluorochromophore: Applications in food quality control. *Food Chemistry*, *119*(2), pp.829-833.

[133]- Wang, Y.T., Bao, Y.J., Lou, L., Li, J.J., Du, W.J., Zhu, Z.Q., Peng, H. and Zhu, J.Z., 2010, November. A novel L-lactate sensor based on enzyme electrode modified with ZnO nanoparticles and multiwall carbon nanotubes. In *SENSORS, 2010 IEEE* (pp. 33-37). IEEE.

[134]- Pachla, L.A., Reynolds, D.L., Wright, D.S. and Kissinger, P.T., 1987. Analytical methods for measuring uric acid in biological samples and food products. *Journal of the Association of Official Analytical Chemists*, *70*(1), pp.01-14.

[135]- Harper, H., 1971. Review of physiological chemistry.

[136]- Nesakumar, N., Thandavan, K., Sethuraman, S., Krishnan, U.M. and Rayappan, J.B.B., 2014. An electrochemical biosensor with nanointerface for lactate detection based on lactate dehydrogenase immobilized on zinc oxide nanorods. *Journal of colloid and interface science*, *414*, pp.90-96.

[137]- Toncev, G., Milicic, B., Toncev, S. and Samardzic, G., 2002. Serum uric acid levels in multiple sclerosis patients correlate with activity of disease and blood–brain barrier dysfunction. *European Journal of Neurology*, *9*(3), pp.221-226.

[138]- Zhang, F.F., Wang, X.L., Ai, S.Y., Sun, Z.D., Wan, Q. and Zhu, Z.Q., 2004. Y, Z, Xian, LT Jin and K. Yamamoto. *Anal. Chim. Acta*, *519*, p.155.

[139]- Wang, Y., Yu, L., Zhu, Z., Zhang, J. and Zhu, J., 2009. Novel uric acid sensor based on enzyme electrode modified by zno nanoparticles and multiwall carbon nanotubes. *Analytical letters*, *42*(5), pp.775-789.

[140]- Lei, Y., Liu, X., Yan, X., Song, Y., Kang, Z., Luo, N. and Zhang, Y., 2012. Multicenter uric acid biosensor based on tetrapod-shaped ZnO nanostructures. *Journal of nanoscience and nanotechnology*, *12*(1), pp.513-518.

[141]- Galbán, J., Andreu, Y., Almenara, M.J., de Marcos, S. and Castillo, J.R., 2001. Direct determination of uric acid in serum by a fluorometric-enzymatic method based on uricase. *Talanta*, *54*(5), pp.847-854.

[142]- Ahmad, R., Tripathy, N., Ahn, M.S., Bhat, K.S., Mahmoudi, T., Wang, Y., Yoo, J.Y., Kwon, D.W., Yang, H.Y. and Hahn, Y.B., 2017. Highly efficient non-enzymatic glucose sensor based on CuO modified vertically-grown ZnO nanorods on electrode. *Scientific reports*, *7*(1), pp.1-10.

[143]- Tzamtzis, N., Psychoyios, V.N., Nikoleli, G.P., Nikolelis, D.P., Psaroudakis, N., Willander, M. and Qadir Israr, M., 2012. Flow potentiometric injection analysis of uric acid using lipid stabilized films with incorporated uricase on ZnO nanowires. *Electroanalysis*, *24*(8), pp.1719-1725.

[144]- Zhao, Y., Yan, X., Kang, Z., Lin, P., Fang, X., Lei, Y., Ma, S. and Zhang, Y., 2013. Highly sensitive uric acid biosensor based on individual zinc oxide micro/nanowires. *Microchimica Acta*, *180*(9-10), pp.759-766.

[145]- Hou, C., Liu, H., Zhang, D., Yang, C. and Zhang, M., 2016. Synthesis of ZnO nanorods-Au nanoparticles hybrids via in-situ plasma sputtering-assisted method for simultaneous electrochemical sensing of ascorbic acid and uric acid. *Journal of Alloys and Compounds*, *666*, pp.178-184.

[146]- Yue, H.Y., Huang, S., Chang, J., Heo, C., Yao, F., Adhikari, S., Gunes, F., Liu, L.C., Lee, T.H., Oh, E.S. and Li, B., 2014. ZnO nanowire arrays on 3D hierachical graphene foam: biomarker detection of Parkinson's disease. *ACS nano*, *8*(2), pp.1639-1646.

[147]- Zhang, X., Zhang, Y.C. and Ma, L.X., 2016. One-pot facile fabrication of graphene-zinc oxide composite and its enhanced sensitivity for simultaneous electrochemical detection of ascorbic acid, dopamine and uric acid. *Sensors and Actuators B: Chemical*, *227*, pp.488-496.

[148]- Liu, H., Gu, C., Hou, C., Yin, Z., Fan, K. and Zhang, M., 2016. Plasma-assisted synthesis of carbon fibers/ZnO core–shell hybrids on carbon fiber templates for detection of ascorbic acid and uric acid. *Sensors and Actuators B: Chemical*, *224*, pp.857-862.

[149]- Chen, J., Zhao, M., Li, Y., Fan, S., Ding, L., Liang, J. and Chen, S., 2016. Synthesis of reduced graphene oxide intercalated ZnO quantum dots nanoballs for selective biosensing detection. *Applied Surface Science*, *376*, pp.133-137.

[150]- Ghanbari, K. and Moloudi, M., 2016. Flower-like ZnO decorated polyaniline/reduced graphene oxide nanocomposites for simultaneous determination of dopamine and uric acid. *Analytical biochemistry*, *512*, pp.91-102.

[151]- Jadon, N., Jain, R., Sharma, S. and Singh, K., 2016. Recent trends in electrochemical sensors for multianalyte detection–A review. *Talanta*, *161*, pp.894-916.

[152]- Ghanbari, K. and Hajheidari, N., 2015. ZnO–CuxO/polypyrrole nanocomposite modified electrode for simultaneous determination of ascorbic acid, dopamine, and uric acid. *Analytical biochemistry*, *473*, pp.53-62.

[153]- Da Silva, J.F. and Williams, R.J.P., 2001. *The biological chemistry of the elements: the inorganic chemistry of life*. Oxford University Press.

[154]- Elinder, F. and Århem, P., 2003. Metal ion effects on ion channel gating. *Quarterly reviews of biophysics*, *36*(4), pp.373-427.

[155]- Asif, M.H., Nur, O., Willander, M. and Danielsson, B., 2009. Selective calcium ion detection with functionalized ZnO nanorods-extended gate MOSFET. *Biosensors and Bioelectronics*, *24*(11), pp.3379-3382.

[156]- Asif, M.H., Nur, O., Willander, M., Yakovleva, M. and Danielsson, B., 2008. Studies on calcium ion selectivity of ZnO nanowire sensors using ionophore membrane coatings. *Research Letters in Nanotechnology*, *2008*.

[157]- Draznin, B., Sussman, K.E., Eckel, R.H., Kao, M., Yost, T. and Sherman, N.A., 1988. Possible role of cytosolic free calcium

concentrations in mediating insulin resistance of obesity and hyperinsulinemia. *The Journal of clinical investigation*, *82*(6), pp.1848-1852.

[158]- Takahashi, T., Neher, E. and Sakmann, B., 1987. Rat brain serotonin receptors in Xenopus oocytes are coupled by intracellular calcium to endogenous channels. *Proceedings of the National Academy of Sciences*, *84*(14), pp.5063-5067.

[159]- Börjesson, S.I., Englund, U.H., Asif, M.H., Willander, M. and Elinder, F., 2011. Intracellular K+ concentration decrease is not obligatory for apoptosis. *Journal of Biological Chemistry*, *286*(46), pp.39823-39828.

[160]- Asif, M.H., Nur, O., Willander, M., Strålfors, P., Brännmark, C., Elinder, F., Englund, U.H., Lu, J. and Hultman, L., 2010. Growth and structure of ZnO nanorods on a sub-micrometer glass pipette and their application as intracellular potentiometric selective ion sensors. *Materials*, *3*(9), pp.4657-4667.

[161]- Asif, M.H., Ali, S.M.U., Nur, O., Willander, M., Englund, U.H. and Elinder, F., 2010. Functionalized ZnO nanorod-based selective magnesium ion sensor for intracellular measurements. *Biosensors and Bioelectronics*, *26*(3), pp.1118-1123.

[162]- Ibupoto, Z.H., Usman Ali, S.M., Chey, C.O., Khun, K., Nur, O. and Willander, M., 2011. Selective zinc ion detection by functionalised ZnO nanorods with ionophore. *Journal of Applied Physics*, *110*(10), p.104702.

[163]- Fulati, A., Usman Ali, S.M., Riaz, M., Amin, G., Nur, O. and Willander, M., 2009. Miniaturized pH sensors based on zinc oxide nanotubes/nanorods. *Sensors*, *9*(11), pp.8911-8923.

[164]- Kumar, N., Senapati, S., Kumar, S., Kumar, J. and Panda, S., 2016, April. Functionalized vertically aligned ZnO nanorods for application in electrolyte-insulator-semiconductor based pH sensors and label-free immuno-sensors. In *Journal of Physics: Conference Series* (Vol. 704, No. 1, p. 012013). IOP Publishing.

[165]- Willander, M. and Al-Hilli, S., 2009. ZnO nanorods as an intracellular sensor for pH measurements. In *Micro and Nano Technologies in Bioanalysis* (pp. 187-200). Humana Press, Totowa, NJ.

[166]- Al-Hilli, S.M., Al-Mofarji, R.T., Klason, P., Willander, M., Gutman, N. and Sa'Ar, A., 2008. Zinc oxide nanorods grown on two-dimensional macroporous periodic structures and plane Si as ap H sensor. *Journal of Applied Physics*, *103*(1), p.014302.

[167]- Maiolo, L., Mirabella, S., Maita, F., Alberti, A., Minotti, A., Strano, V., Pecora, A., Shacham-Diamand, Y. and Fortunato, G., 2014. Flexible pH sensors based on polysilicon thin film transistors and ZnO nanowalls. *Applied physics letters*, *105*(9), p.093501.

[168]- Zhang, Q., Liu, W., Sun, C., Zhang, H., Pang, W., Zhang, D. and Duan, X., 2015. On-chip surface modified nanostructured ZnO as functional pH sensors. *Nanotechnology*, *26*(35), p.355202.

[169]- Zhang, F., Wang, X., Ai, S., Sun, Z., Wan, Q., Zhu, Z., Xian, Y., Jin, L. and Yamamoto, K., 2004. Immobilization of uricase on ZnO nanorods for a reagentless uric acid biosensor. *Analytica Chimica Acta*, *519*(2), pp.155-160.

[170]- Al-Hilli, S.M., Al-Mofarji, R.T. and Willander, M., 2006. Zinc oxide nanorod for intracellular p H sensing. *Applied physics letters*, *89*(17), p.173119.

[171]- Kang, B.S., Ren, F., Heo, Y.W., Tien, L.C., Norton, D.P. and Pearton, S.J., 2005. p H measurements with single ZnO nanorods integrated with a microchannel. *Applied physics letters*, *86*(11), p.112105.

[172]- Wang, J.L., Yang, P.Y., Hsieh, T.Y. and Juan, P.C., 2015. Ionic pH and glucose sensors fabricated using hydrothermal ZnO nanostructures. *Japanese Journal of Applied Physics*, *55*(1S), p.01AE16.

[173]- Wang, J.L., Yang, P.Y., Hsieh, T.Y., Hwang, C.C. and Juang, M.H., 2013. pH-sensing characteristics of hydrothermal Al-doped ZnO nanostructures. *Journal of Nanomaterials*, *2013*.

[174]- Lee, S.C., Hamilton, J.S., Trammell, T.R.A.C.Y., Horwitz, B.A. and Pappone, P.A., 1994. Adrenergic modulation of intracellular pH in isolated brown fat cells from hamster and rat. *American Journal of Physiology-Cell Physiology*, *267*(2), pp.C349-C356.

[175]- Yates, D.E., Levine, S. and Healy, T.W., 1974. Site-binding model of the electrical double layer at the oxide/water interface. *Journal of the Chemical Society, Faraday Transactions 1: Physical Chemistry in Condensed Phases*, *70*, pp.1807-1818.

[176]- Yang, K., She, G.W., Wang, H., Ou, X.M., Zhang, X.H., Lee, C.S. and Lee, S.T., 2009. ZnO nanotube arrays as biosensors for glucose. *The Journal of Physical Chemistry C*, *113*(47), pp.20169-20172.

[177]- Tarlani, A., Fallah, M., Lotfi, B., Khazraei, A., Golsanamlou, S., Muzart, J. and Mirza-Aghayan, M., 2015. New ZnO nanostructures as non-enzymatic glucose biosensors. *Biosensors and Bioelectronics*, *67*, pp.601-607.

[178]- Yang, Y., Wang, Y., Bao, X. and Li, H., 2016. Electrochemical deposition of Ni nanoparticles decorated ZnO hexagonal prisms as an effective platform for non-enzymatic detection of glucose. *Journal of Electroanalytical Chemistry*, *775*, pp.163-170.

[179]- Liu, Y., Pang, H., Wei, C., Hao, M., Zheng, S. and Zheng, M., 2014. Mesoporous ZnO-NiO architectures for use in a high-performance nonenzymatic glucose sensor. *Microchimica Acta*, *181*(13-14), pp.1581-1589.

[180]- Cai, B., Zhou, Y., Zhao, M., Cai, H., Ye, Z., Wang, L. and Huang, J., 2015. Synthesis of ZnO–CuO porous core–shell spheres and their application for non-enzymatic glucose sensor. *Applied physics A*, *118*(3), pp.989-996.

[181]- Soejima, T., Takada, K. and Ito, S., 2013. Alkaline vapor oxidation synthesis and electrocatalytic activity toward glucose oxidation of CuO/ZnO composite nanoarrays. *Applied surface science*, *277*, pp.192-200.

[182]- Fatemi, H., Khodadadi, A.A., Firooz, A.A. and Mortazavi, Y., 2012. Apple–biomorphic synthesis of porous ZnO nanostructures for glucose direct electrochemical biosensor. *Current Applied Physics*, *12*(4), pp.1033-1038.

[183]- Ridhuan, N.S., Razak, K.A. and Lockman, Z., 2018. Fabrication and characterization of glucose biosensors by using hydrothermally grown ZnO nanorods. *Scientific reports*, *8*(1), pp.1-12.

[184]- Israr, M.Q., Sadaf, J.R., Asif, M.H., Nur, O., Willander, M. and Danielsson, B., 2010. Potentiometric cholesterol biosensor based on ZnO nanorods chemically grown on Ag wire. *Thin solid films*, *519*(3), pp.1106-1109.

[185]- Lu, Y.M., Wang, P.C., Tang, J.F. and Chu, S.Y., 2017. Dependence of seed layer thickness on sensitivity of nano-ZnO cholesterol biosensor. In *IOP Conference Series: Materials Science and Engineering* (Vol. 167, No. 1, p. 012021). IOP Publishing.

[186]- Ma, S., Zhang, X., Liao, Q., Liu, H., Huang, Y., Song, Y., Zhao, Y. and Zhang, Y., 2015. Enzymatic lactic acid sensing by In-doped ZnO nanowires functionalized AlGaAs/GaAs high electron mobility transistor. *Sensors and Actuators B: Chemical*, *212*, pp.41-46.

[187]- Zhao, Y., Yan, X., Kang, Z., Fang, X., Zheng, X., Zhao, L., Du, H. and Zhang, Y., 2014. Zinc oxide nanowires-based electrochemical biosensor for L-lactic acid amperometric detection. *Journal of nanoparticle research*, *16*(5), pp.1-9.

[188]- Alam, F., Jalal, A.H., Sinha, R., Umasankar, Y., Bhansali, S. and Pala, N., 2018. Sonochemically synthesized ZnO nanostructure-based L-lactate enzymatic sensors on flexible substrates. *MRS Advances*, *3*(5), pp.277-282.

[189]- Ahmad, R., Tripathy, N., Ahn, M.S. and Hahn, Y.B., 2017. Solution process synthesis of high aspect ratio ZnO nanorods on electrode surface for sensitive electrochemical detection of uric acid. *Scientific reports*, *7*(1), pp.1-8.

[190]- Ali, S.M.U., Ibupoto, Z.H., Kashif, M., Hashim, U. and Willander, M., 2012. A potentiometric indirect uric acid sensor based on ZnO nanoflakes and immobilized uricase. *Sensors*, *12*(3), pp.2787-2797.

[191]- Ahmad, R., Tripathy, N., Jang, N.K., Khang, G. and Hahn, Y.B., 2015. Fabrication of highly sensitive uric acid biosensor based on directly grown ZnO nanosheets on electrode surface. *Sensors and Actuators B: Chemical*, *206*, pp.146-151.

[192]- Song, Y., Zhang, X., Yan, X., Liao, Q., Wang, Z. and Zhang, Y., 2014. An enzymatic biosensor based on three-dimensional ZnO nanotetrapods spatial net modified AlGaAs/GaAs high electron mobility transistors. *Applied Physics Letters*, *105*(21), p.213703.

[193]- Ali, M., Shah, I., Kim, S.W., Sajid, M., Lim, J.H. and Choi, K.H., 2018. Quantitative detection of uric acid through ZnO quantum dots based highly sensitive electrochemical biosensor. *Sensors and Actuators A: Physical*, *283*, pp.282-290.

[194]- Lokman, A., Harun, S.W., Harith, Z., Rafaie, H.A., Nor, R.M. and Arof, H., 2015. Inline Mach–Zehnder interferometer with ZnO nanowires coating for the measurement of uric acid concentrations. *Sensors and Actuators A: Physical*, *234*, pp.206-211.

[195]- Asif, M.H., Fulati, A., Nur, O., Willander, M., Brännmark, C., Strålfors, P., Börjesson, S.I. and Elinder, F., 2009. Functionalized zinc oxide nanorod with ionophore-membrane coating as an intracellular Ca 2+ selective sensor. *Applied Physics Letters*, *95*(2), p.023703.

[196]- Ali, S.M.U., Asif, M.H., Fulati, A., Nur, O., Willander, M., Brännmark, C., Strålfors, P., Englund, U.H., Elinder, F. and Danielsson, B., 2010. Intracellular $K^+$ Determination With a Potentiometric Microelectrode Based on ZnO Nanowires. *IEEE transactions on nanotechnology*, *10*(4), pp.913-919.

[197]- Khun, K., Ibupoto, Z.H., Chey, C.O., Lu, J., Nur, O. and Willander, M., 2013. Comparative study of ZnO nanorods and thin films for chemical and biosensing applications and the development of ZnO nanorods based potentiometric strontium ion sensor. *Applied surface science*, *268*, pp.37-43.

[198]- Wahab, H.A., Salama, A.A., El-Saeid, A.A., Nur, O., Willander, M. and Battisha, I.K., 2013. Optical, structural and morphological studies of (ZnO) nano-rod thin films for biosensor applications using sol gel technique. *Results in Physics*, *3*, pp.46-51.

[199]- Ibupoto, Z.H., Ali, S.M.U., Khun, K. and Willander, M., 2012. Selective thallium (I) ion sensor based on functionalised ZnO nanorods. *Journal of Nanotechnology*, *2012*.

[200]- Van Thanh, P., Mai, H.H., Tuyen, N.V., Doanh, S.C. and Viet, N.C., 2017. Zinc oxide nanorods grown on printed circuit board for extended-gate field-effect transistor pH sensor. *Journal of Electronic Materials*, *46*(6), pp.3732-3737.

[201]- Huang, B.R., Lin, J.C. and Yang, Y.K., 2013. ZnO/Silicon nanowire hybrids extended-gate field-effect transistors as pH sensors. *Journal of the Electrochemical Society*, *160*(6), p.B78.

[202]- Young, S.J., Lai, L.T. and Tang, W.L., 2019. Improving the performance of pH sensors with one-dimensional ZnO nanostructures. *IEEE Sensors Journal*, *19*(23), pp.10972-10976.

[203]- Zhou, F., Jing, W., Liu, S., Mao, Q., Xu, Y., Han, F., Wei, Z. and Jiang, Z., 2020. Electrodeposition of gold nanoparticles on ZnO nanorods for improved performance of enzymatic glucose sensors. *Materials Science in Semiconductor Processing*, *105*, p.104708.

[204]- Mao, Q., Jing, W., Zhou, F., Liu, S., Gao, W., Wei, Z. and Jiang, Z., 2021. Depositing reduced graphene oxide on ZnO nanorods to improve the performance of enzymatic glucose sensors. *Materials Science in Semiconductor Processing*, *121*, p.105391.

[205]- Khan, M., Nagal, V., Masrat, S., Tuba, T., Tripathy, N., Parvez, M.K., Al-Dosari, M.S., Khosla, A., Furukawa, H., Hafiz, A.K. and Ahmad, R., 2022. Wide-Linear Range Cholesterol Detection Using Fe2O3 Nanoparticles Decorated ZnO Nanorods Based Electrolyte-Gated Transistor. *Journal of The Electrochemical Society*, *169*(2), p.027512.

[206]- Alam, F., Jalal, A.H., Forouzanfar, S., Karabiyik, M., Baboukani, A.R. and Pala, N., 2020. Flexible and linker-free enzymatic sensors based on zinc oxide nanoflakes for noninvasive L-lactate sensing in sweat. *IEEE Sensors Journal*, *20*(10), pp.5102-5109.

[207]- Nien, Y.H., Kang, Z.X., Su, T.Y., Ho, C.S., Chou, J.C., Lai, C.H., Kuo, P.Y., Lai, T.Y., Dong, Z.X., Chen, Y.Y. and Huang, Y.H., 2021. Investigation of flexible arrayed lactate biosensor based on copper doped zinc oxide films modified by iron–platinum nanoparticles. *Polymers*, *13*(13), p.2062.

[208]- Nagal, V., Kumar, V., Khan, M., AlOmar, S.Y., Tripathy, N., Singh, K., Khosla, A., Ahmad, N., Hafiz, A.K. and Ahmad, R., 2021. A highly sensitive uric acid biosensor based on vertically arranged ZnO nanorods on a ZnO nanoparticle-seeded electrode. *New Journal of Chemistry*, *45*(40), pp.18863-18870.

[209]- Hamid, H.A., Lockman, Z., Nor, N.M., Zakaria, N.D. and Razak, K.A., 2021. Sensitive detection of Pb ions by square wave anodic stripping voltammetry by using iron oxide nanoparticles decorated zinc oxide nanorods modified electrode. *Materials Chemistry and Physics*, *273*, p.125148.

[210]- Young, S.J., Chu, Y.J. and Chen, Y.L., 2021. Enhancing pH sensors performance of ZnO nanorods with Au nanoparticle's adsorption. *IEEE Sensors Journal*, *21*(12), pp.13068-13073.

[211]- Chu, Y.L., Young, S.J., Dai, H.R., Lee, Y.M., Khosla, A., Chu, T.T. and Ji, L.W., 2021. Improved pH-sensing characteristics by Pt nanoparticle-decorated ZnO nanostructures. *ECS Journal of Solid-State Science and Technology*, *10*(6), p.067001.